2012

Characterization of NanoGUMBOS for future electronic devices

Naveen Narayan Jagadish
Louisiana State University and Agricultural and Mechanical College

CHARACTERIZATION OF NANOGUMBOS FOR FUTURE ELECTRONIC DEVICES

A Thesis
Submitted to the Graduate Faculty of the
Louisiana State University and
Agricultural and Mechanical College
in partial fulfillment of
the requirements for the degree of
Master of Science in Electrical Engineering
in
The Department of Electrical and Computer Engineering

By
Naveen Narayan Jagadish
B.E, Visvesvaraya Technological University, India, 2007
May 2012

To my parents and brother,

Jagadish K. Narayan,

Uma N. Jagadish,

Sachin N. Jagadish

ACKNOWLEDGEMENTS

First and foremost, I offer my sincere gratitude to my advisor, Dr. Theda Daniels-Race, for her invaluable support, encouragement and guidance for the successful completion of my thesis. I am indebted to her for giving me an opportunity to explore new ideas and helping me to implement them.

It was an honor to have Dr.Martin Feldman and Dr.DooYoung Hah on my thesis committee. I thank them for their help, patience, and support throughout this process.

I would like to express my gratitude to Dr.Warner, Dept of Chemistry, LSU and his students Mr.Sergio DeRooy, Ms.Atiya Jordan and Ms.Ashleigh Wright for providing GUMBOS samples for this project.

I am thankful for Mr.Golden Hwaung for helping me in the laboratory. I sincerely thank Dr.A.Kelley for assistance with conductive probe atomic force microscopy measurements. I am also grateful to Mr.Naga, Mr.Kalyan and Mr.Chiranjth for their suggestions that helped me to pursue my research with great confidence. I acknowledge the support from Public Policy Research Lab, LSU for partially funding my Masters' degree.

I acknowledge support from the Louisiana Board of Regents (LEQSF(2011-14)-RD-A-07), the National Science Foundation ((2010)-PFUND-172), NASA (DART-44) and Dr. Kristina Johnson via the LSU Foundation (F017).

Finally, I thank my parents and my brother for their love and support, without which I would not have accomplished this work.

TABLE OF CONTENTS

LIST OF TABLES

LIST OF FIGURES

ABSTRACT

In our work on hybrid (organic-inorganic) electronic materials (HEMs), we have developed a reasonably facile method for characterizing GUMBOS or a Group of Uniform Materials Based on Organic Salts. In addition to the versatility of traditional ionic liquids (i.e.-solubility, melting point, viscosity), NanoGUMBOS are functionalizable to exhibit properties such as fluorescence, magnetic susceptibility, and even antimicrobial activity. However, given our interest in the electrical properties of HEMs, we have made first-time measurements of NanoGUMBOS, using *conductive probe Atomic Force Microscopy* (CP-AFM), in order to deduce their room temperature current-voltage characteristics. In conjunction with the nanoscale imaging of AFM alone, we have observed both the morphology and conductivity of these unique materials. Our results bode well for combining GUMBOS with substrates of more traditional materials, such as metals or semiconductors, to serve as the basis for future HEMs-based devices. We have also determined the optical characteristics of NanoGUMBOS using *Raman Spectroscopy (RS)*. The Raman signatures can be used for detection of a nanoparticle and modeling the electron-phonon interaction inside the nanoparticle.

1. INTRODUCTION

1.1 Research Goals

As semiconductor technology faces the limits of Moore's law,[†] there is a widespread endeavor to scale down transistor size while maintaining a cost-effective trajectory and improvement in the performance of integrated circuits (ICs). [1][2] As a result, new fabrication methodologies and materials are being explored by researchers worldwide.

Over the last decade, Hybrid Electronic Materials (HEMs), which are made by combining organic and inorganic electronic materials, have shown promise as eligible candidates for next generation devices. Although ongoing work in areas such as organic semiconductors (i.e.-flexible electronics) has yielded promising results, [3-5] the successful integration of molecular species with traditional inorganic materials, such as metals or semiconductors, is still a challenge. Toward this end, we have taken up the task of investigating a literally new form of electronic material known as GUMBOS or a **G**roup of **U**niform **M**aterials **B**ased on **O**rganic **S**alts (GUMBOS) to understand their potential as core components for future HEMs based devices. Introduced to the literature in 2008 by Professor Isiah M. Warner of the LSU Department of Chemistry, GUMBOS represent first-time synthesis of nanoparticles (or NanoGUMBOS) from frozen ionic liquids. [6] In terms of both structure and function the versatility of GUMBOS is extensive as the Warner Group has successfully synthesized these materials in the form of nanoparticles/nanowires/nanorods which, in turn, have exhibited properties of fluorescence, magnetic susceptibility, and even antimicrobial activity. GUMBOS also have high ionic conductivity and high thermal stability which are properties essential to even proof-of principle consideration of organic-inorganic materials integration. Thus, in order

[†] Moore's Law states that "The number of transistors on a chip doubles every two years." [2]

to ascribe NanoGUMBOS/HEMs to emerging electronic materials, the fundamental step is to determine their electronic and/or optical properties. This thesis is focused upon the characterization of different types of NanoGUMBOS using Atomic Force Microscopy (AFM) and Raman Spectroscopy to investigate electrical and optical properties, respectively.

Electrical characterization is carried out by a method known as *Conductive Probe Atomic Force Microscopy* (CP-AFM). In this method, an electrically conductive tip is used as one contact electrode and a gold surface as the other. The GUMBOS nanoparticles are incorporated onto the gold surface, and a closed circuit is formed by bringing the tip in contact with the nanoparticles. Current is passed and measured using an external circuit, and current-voltage (I-V) plots are obtained. This method allows for the determination of other electrical parameters of interest such as conductivity (or resistivity) when applied to GUMBOS in nanowire form.

The optical characterization of GUMBOS is accomplished using Raman Spectroscopy. Spectral signatures for different species of NanoGUMBOS are obtained, and their Raman peaks are correlated with the molecular structure and chemical bonding of the material. Information of this form is important for not only structural verification but, in turn, may be of use to studies of phenomena (i.e.-electron phonon interactions) important to future HEMs device development.

1.2 Review of Literature

1.2.1 Background

'Nano' meaning 'dwarf' in Greek may be a simple prefix. Ironically, nanotechnology, which in essence is an interdisciplinary science that deals with the effect of size upon the properties of the material or structure under study, has made "giant" contributions to electronics technology. Over the last two decades, in particular, nanotechnology has revolutionized advancements in areas such as communications, energy, and even medicine, to name a few, and

as such, has improved the standard of living. [7-9] Our research falls within the domain of nanoelectronics which, in turn, encompasses the study of fundamental electronic devices such as the transistor in the nanoscale. With respect to HEMs especially, we approach nanotechnology from the perspective of utilizing the very molecular structure of materials to investigate their resultant characteristics and potential device applications. However, as mentioned, the very breadth, let alone the depth of nanoscience/nanotechnology, is as such that a comprehensive review of the literature is the subject of copious books and journal series. [10-12] Therefore, in this section of this thesis, we first provide a basic overview of the evolution of nanoelectronics. We focus our discussion on a review of selected discoveries, techniques and proofs-of-concept for nano materials and structures as may be considered pertinent to the steps leading to our work.

1.2.2 Overview of Nanoelectronics

Nanoelectronics describes the field in which molecules or nanoparticles are utilized as basic elements in making electronic devices. In nanoelectronics, there are two fundamental approaches for making electronic components— the "top-down" approach which involves shrinking from macro scale to nano scale and the "bottom-up" approach where single molecules, a group of molecules or nanostructures are used to make electronic components. The top-down approach has been the primary methodology for large scale fabrication of chips i.e., photolithography of silicon for making large numbers of *complementary metal oxide semiconductor* (CMOS) transistors. In nanoelectronics, the devices are made at the nanoscale level or a group of molecules are exploited for any kind of device behavior like a resistor, diode, or transistor. In 1959, Richard Feynman's famous lecture on 'There's Plenty of Room at the Bottom' gave hope to researchers in terms of the future manipulation of physical properties at the atomic level. [7] However, it was as early as 1974 when Aviram and Ratner published their

now seminal article on “Molecular rectifiers,” which described their theoretical ideas on using organic molecules as rectifiers in electronic circuits, that later became known as “molecular electronics” or *hybrid electronic materials* (HEMs) emerged. [3]

The biggest challenges that have been faced in bottom-up molecular electronics are the difficulties in handling and manipulation of molecules and their viability for large scale device manufacturing. However, the invention of the Scanning Tunneling Microscope in 1981 by Benning and Roher, gave hope for manipulation and electrical measurements at the nanoscale. [13] Although top-down photolithography has been the primary method employed in large scale chip manufacturing, the interesting properties of molecules have driven researchers to find alternatives to the existing *complementary metal oxide semiconductor* (CMOS) technology. For example, Figure 1.1 shows the design of an organic field effect transistor (FET). [14] In this design, a conducting polymer called Polythiophene was utilized as a semiconductor. An n-type silicon wafer with oxide layer on the top was used as the substrate and two gold electrodes were connected to source and drain. This transistor behavior was similar to that of a conventional MOSFET and also showed that organic macromolecules are promising candidates for future devices.

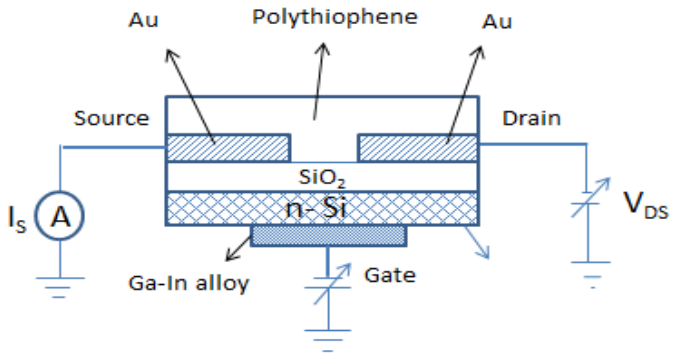

Figure 1.1: Cross-sectional view of the organic field effect transistor (FET). Reprinted from [14].

In 1975, Gordon E. Moore, a co-founder of Intel Corporation, made a prediction that the transistor count on a single chip would increase by a factor of two every 24 months. Figure 1.2 shows the estimation known as Moore's law which has become a business-dictum for the entire semiconductor industry. [2] [15]

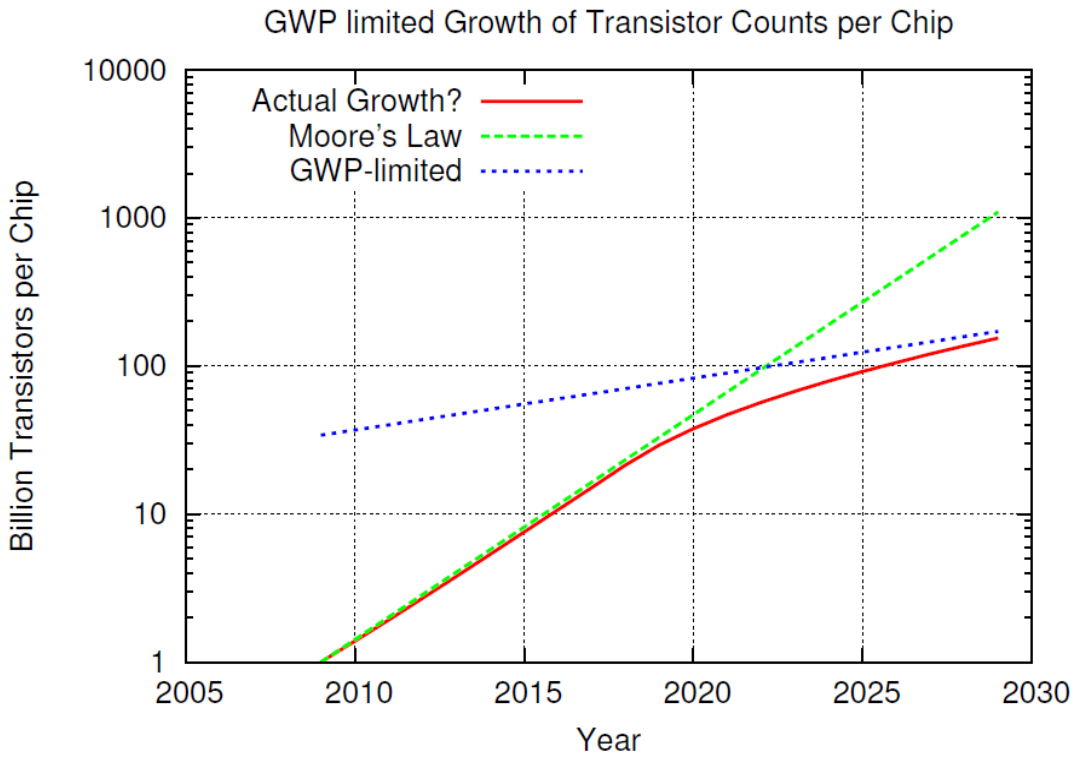

Figure 1.2: Moore's Law prediction, Actual Growth and Gross World Product (GWP). Reprinted with permission from [15]. [Appendix A]

In 1998, semiconductor companies from the leading chip manufacturing regions—Europe, Japan, Korea, Taiwan, and the United States—joined together to create the *International Technological Roadmap of Semiconductors* (ITRS) to ensure the time-cost mutuality envisioned by Moore. [1] Every year, this consortium of experts produces a review document on new fabrication methodologies and materials that have the potential to replace existing technology. There is also a need for these experts to consider the economic limit to Moore's law. As the

transistor density is increasing, the selling price of a single chip is decreasing. However, for every new generation, the production costs become more expensive although this trend is limited by the Gross World Product (GWP). Nonetheless, the evolution of the "simple" transistor toward the nanotechnological realm has undergone remarkable changes and advancements in the past several decades. We provide a selective overview of these developments in the discussion to follow.

Towards miniaturization of electronic components, improvements in lithography techniques on silicon (which has been the primary material for making transistors for semiconductor industry) are reaching the level of saturation. Many limitations like controlling heat dissipated from large numbers of transistors and leakage mechanisms like short-channel effects leading to device failure are being faced. [12] Also, with the current size of a single transistor being 16nm, [1] challenges like creating defect free masks using Extreme Ultraviolet (EUV) lithography, use of optimal photoresist and source brightness, and the need for improvement in maskless lithography techniques for increased throughput are ongoing. Thus, there is a need for alternative materials and techniques to overcome these challenges and to provide solutions for making future electronics devices.

Arguably, nanowires are the most commonly used nanostructures in nanoelectronics. Nanowires are used as building blocks in making complex devices (e.g. electrical contacts) and in some direct applications (e.g. diodes). Gate-all-around FETs with nanowires as channels have proven to be superior compared to silicon based MOSFETs. [16] In 2003, Meyyappan et.al successfully demonstrated multilevel data storage based on nanowire transistors as shown in Figure 1.3. [17] In this device nanowires with self-assembled redox molecules acted as a

channel. As opposed to standard single bit per cell technology, this device had three bits per cell enabling eight levels.

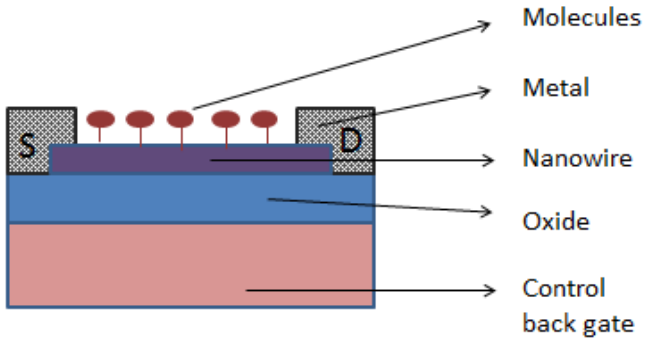

Figure 1.3: Multilevel molecular memory demonstrated by Meyyappan et.al.
Reprinted from [17]

As are most directly related to the research of this thesis, characterization techniques have played a significant role in nanoelectronics. The invention of the Atomic Force Microscope (AFM) in 1986, revolutionized nanoelectronics as it enabled imaging, manipulation and characterization at the nanoscale level. [18-20] AFM provides non-damaging high resolution images of surfaces and can also be used to extract electric, magnetic and other properties of nanostructures. Other metrology tools like Raman Spectroscopy (RS) are employed to extract optical properties. These characterization techniques are useful in studying the flow of electrons and electron-phonon interaction within a nanostructure, thereby providing viable information for future device development.

The first time use of Scanning Tunneling Microscopy (STM) for electrical measurements on molecules was done by Xu et al., [21] in 2003, in which they measured the conductance of a single molecule. Several gold-molecule-gold junctions were formed by repeatedly bringing a gold tip into and out of contact with the gold electrode immersed in a solution. This technique, which is also known as STM-controlled break junction, gave robust results as large number of

measurements was possible on the same types of molecules. Figure 1.4 illustrates STM-controlled break junction formation.

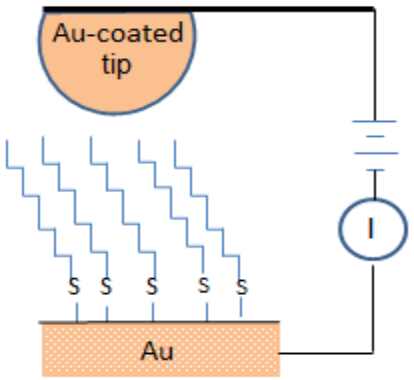

Figure 1.4: Electrical measurements made using STM by Xu et al. [21]

Over the last decade, conductive probe AFM (CP-AFM) has become one of the most preferred metrological tools for electrical measurements at the nanoscale. [22-26] In CP-AFM, a conductive tip is used as one of the electrodes. Some important and relevant works include CP-AFM measurements on Fe_2O_3 nanowires by Hsu et al [27], bismuth sulfide nanowire arrays by Birjukovs et al [28] and HgTe nanowires by Gunderson et al [29]. Figure 1.5 shows the implementation of CP-AFM on Fe_2O_3 nanowires. In this technique, Fe_2O_3 nanowires were grown on a conductive indium tin oxide (ITO) glass coated with Fe_2O_3 film. A conductive Au-coated silicon tip was used as one of the electrodes and ITO base as the other. This technique was successfully used to measure electrical activity in the structure shown.

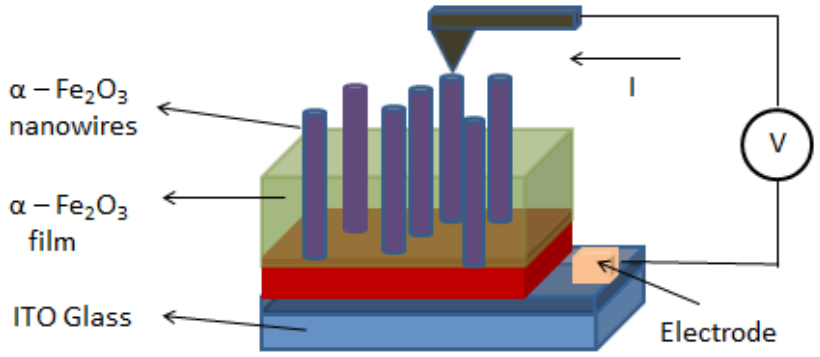

Figure 1.5: Conductive atomic force microscopy on Fe_2O_3 nanowires. Reprinted with permission from [27]. [Appendix A]

About three decades ago, the phenomenon of Surface Enhanced Raman spectroscopy (SERS) was observed with molecules on metal surfaces. [30][31] However, it was twenty years later that SERS was first used as a tool to detect molecules of interest. In 1977, Shuming et al first demonstrated the detection of single molecules and single nanoparticles using SERS. [32] Their methods also opened doors for studying size-dependent properties of nanostructures. Since then, the field of SERS has grown drastically, enabling selective detection of molecules and nanoparticles. SERS also enables the study of optical properties within the nanostructures. Determination of vibrational states of molecules (phonons) helps in understanding the electron-phonon interaction inside the nanostructure. Thus, SERS can be considered an important characterization tool for modeling nanoscale opto-electronic devices.

1.3 Challenges and Limitations in This Work

The electrical characterization is accomplished by a technique known as *Conductive Probe Atomic Force Microscopy* (CP-AFM). In this method, an electrically conductive tip is used as one of the electrodes and a gold surface as the other. Nanoparticles are incorporated onto the gold surface and a closed circuit is formed by bringing the tip in contact with the

nanoparticles. Current is passed and measured using an external circuit, and current-voltage (I-V) plots are obtained for use in the determination of resistivity and conductivity values.

In the case of CP-AFM, the difficulty lies in placing the tip above the nanoparticle. Also, the tip has to be replaced frequently due to wear during scanning (see Appendix B). Although a good conductor, the gold surface itself, being one of the electrodes, contributes to some contact resistance. Finally, the sizes of the nanoparticles vary with one another, and thus sample dimensions must be estimated over an average collection of particles.

The optical characterization of nanowires is performed using Raman Spectroscopy (RS). The spectral signatures of different species of NanoGUMBOS are obtained and peaks are correlated with the molecular structure and chemical bonding of the material. The spectral information of these nanoparticles will help with the correlation of certain types of GUMBOS to certain properties as derived from the electron–phonon interaction within these materials.

However, one of the challenges faced in the use of RS stems from the fluorescence of the material itself. If the material of interest exhibits fluorescence, the intensity of the scattered signal from the sample increases, thereby affecting the Raman spectra. Other difficulties include selecting a suitable surface, eliminating impurities on the surface and focusing the laser precisely on the nanoparticle.

1.4 Organization of Thesis:

Chapter 1 has given a selected overview of nanoelectronic research as motivated by the need to scale down electronic components. Chapter 2 describes the special properties of GUMBOS as these materials were the subject of our characterization studies. Chapter 3 discusses the characterization of NanoGUMBOS using conductive probe atomic force

microscopy (CP-AFM). Chapter 4 presents the spectral signatures of some types of NanoGUMBOS taken using Raman Spectroscopy (RS).

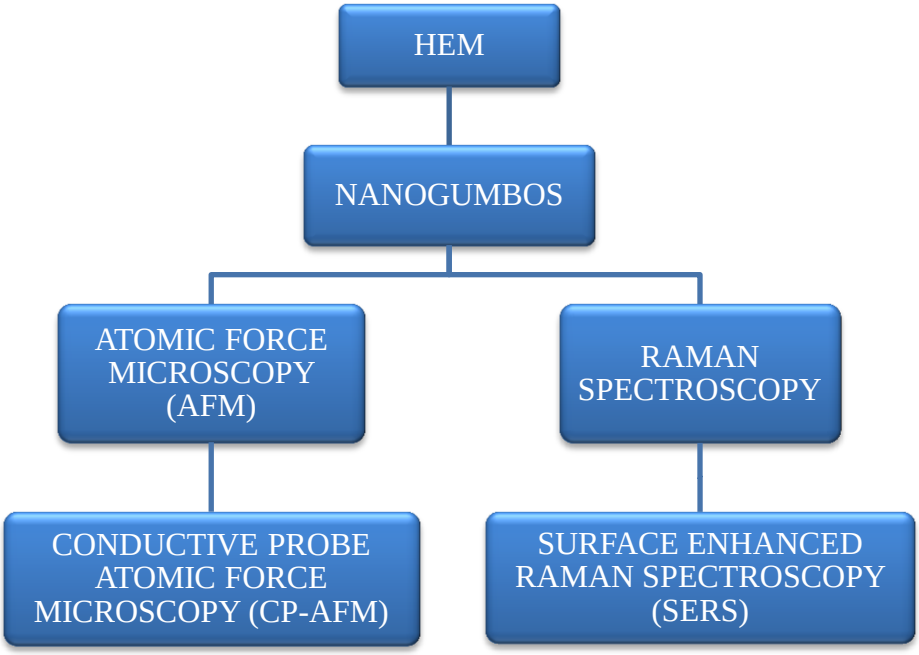

Figure 1.6: Characterization Hierarchy.

Finally, with GUMBOS being such a "new" material, and with the emphasis upon characterization in this thesis, we provide Figure 1.6 as a guide to the approach taken in our investigation.

2. GUMBOS AND THEIR CHARACTERISTICS

2.1 Introduction

GUMBOS, a *Group of Uniform Materials based on Organic Salts*, represent a first-time synthesis of nanoscale material composed of ionic liquid species in the frozen (solid) state. GUMBOS have high ionic conductivity, high thermal stability and are broadly tunable, which are all useful characteristics for electronic materials. GUMBOS were first synthesized by Dr. Isiah M.Warner and his group in 2008. [6] Since then, this special category of particles has shown promise as potential candidates in various applications such as device electronics, sensors, displays, fuel cells, and medical imaging. [33][34] Compared to VOCs (volatile organic compounds), GUMBOS can be functionalized to have minimal (if any) negative environmental effects and are thus preferable for use in various applications as described above. However, as this is effectively a "new" class of materials, prior to this work little was known about their electrical properties. Thus, our research represents a first-time investigation of the electronic characteristics of GUMBOS and their potential utilization in hybrid electronic materials (HEMs) and device structures.

2.2 Characteristics of Ionic Liquids and GUMBOS

Traditional ionic liquids (ILs) are categorized into two main types -RTIL (room temperature ionic liquids) and Frozen (solid state) Ionic Liquids. [35-37] Ionic liquids generally have the following properties:

- High ionic conductivity
- Non-volatile
- High thermal stability/Low vapor pressure
- Highly solvating for organic, inorganic, hydrophobic and hydrophilic materials

● Recyclable (also known as “green solvents”)

● Broadly tunable (i.e.-solubility, melting point, viscosity)

Typically, traditional ILs have melting points in the range from room temperature (~25˚C) up to 100˚C. However, one of the unique and particularly significant properties of GUMBOS is their extended range of melting points up to 250˚C. [38] This “frozen” or solid-state, in addition to the achievement of nanoparticle synthesis, defines GUMBOS as an effectively “new” material in terms of IL research with properties as follows:

● Size and properties mimic traditional nanoparticles.

● Scalable – nanoparticle size can be controlled.

● Functionalizable – also called “designer nanoparticles” as they can be modified for task-specific properties – e.g. - fluorescence, magnetic susceptibility, antimicrobial activity, chirality, and electrical properties.

Thus, from the electrical engineering perspective and therefore for our purposes, we consider GUMBOS as an opportunity in the realm of HEMs and hybrid electronic devices (HEDs).

2.3 Preparation of NanoGUMBOS

GUMBOS as nanoparticles, or NanoGUMBOS, represent a paradigm shift in nanoparticle construction and applications. The first samples were prepared from frozen ionic liquids by a procedure based on what is known as the *oil-in-water (o/w) micro-emulsion-quench* approach. [6] As described in the 2008 NanoLetters publication of Tesfai *et al*. from the Warner Group, this approach involves two methods in which, *1-butyl-2, 3-dimethylimidazolium hexafluorophosphate* [bm2Im][PF6], an IL with a melting point of 42 °C, is used as the raw material. The procedure of micro-emulsion-quench approach is illustrated in Figure 2.1. In the first method [bm2Im][PF6] is melted in water followed by o/w dispersion in water maintained above the IL’s melting point and then rapid cooling which forms the nanoparticles. In the second

method, an emulsifier and nonionic surfactant called *Brij 35* is used to form the nanoparticles. The molten [bm2Im][PF6] is added drop by drop to the surfactant solution followed by homogenization and probe sonication. Finally the particles are solidified by rapid quenching in an ice bath. In this approach, the size of the nanoparticle depends on the processing conditions. The sizes of the nano and micro particles formed by this process vary from 60nm to 120nm.

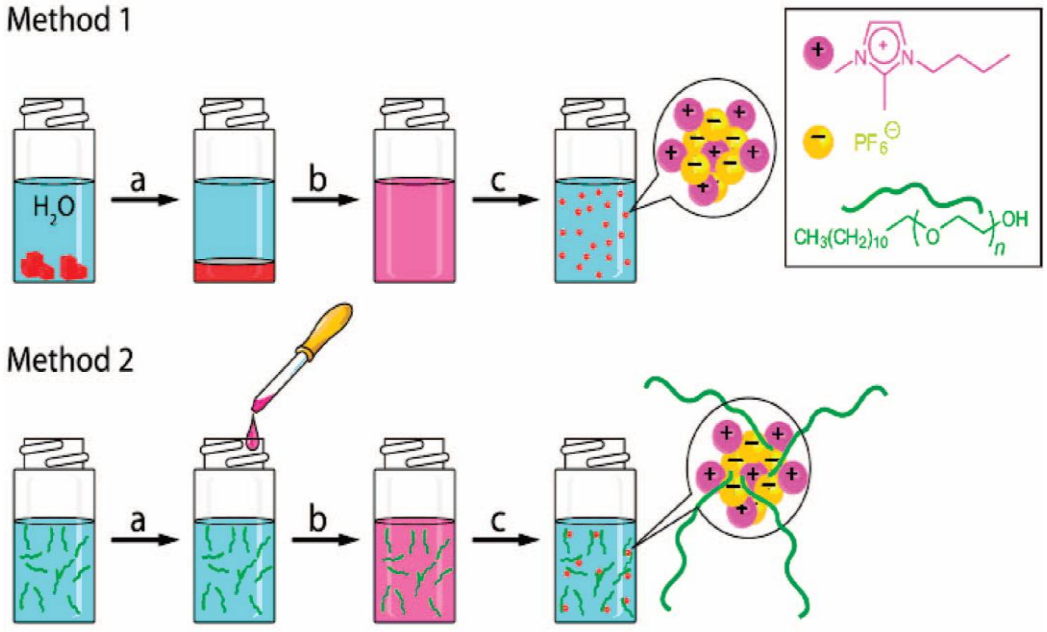

Figure 2.1: Schematic of melt-emulsion-quench procedure showing two methods – Using Surfactantless (method 1) and Surfactant-Assisted (method 2). [Appendix A]

Other methods to produce the nanoparticles from GUMBOS include- 1) In-situ ion exchange, 2) anion exchange, 3) reprecipitation and 4) aerosol generation. In our work, we have characterized different types of NanoGUMBOS made from the anion exchange method or the reprecipitation method. The anion exchange procedure involves ion-association of a hydrophilic cationic dye and a hydrophobic anion to form NanoGUMBOS. [39] In the reprecipitation method, NanoGUMBOS are formed by the addition of 150 µL of a 1 mM ethanolic solution of GUMBOS to 5 mL of DI water under sonication for 5 minutes. [40]

2.3.1 Preparation of One Dimensional NanoGUMBOS

One-dimensional (1D) organic nanostructures have potential applications in electronics for Organic Light Emitting Diodes (OLEDs), Organic Field effect Transistors (OFETs) and optoelectronics. In Prof. Warner's laboratory, a facile templating method is employed to prepare one-dimensional NanoGUMBOS. [39] In this method, a commercially available anodic aluminum oxide (AAO) membrane (which has nanopores) is used as a template as shown in Figure 2.2. The minute pores in this AAO membrane are filled with the saturated solution of GUMBOS and allowed to dry for 12 hours. After solidification, the membrane is etched off using 0.5 M phosphoric acid solution to form nanowires.

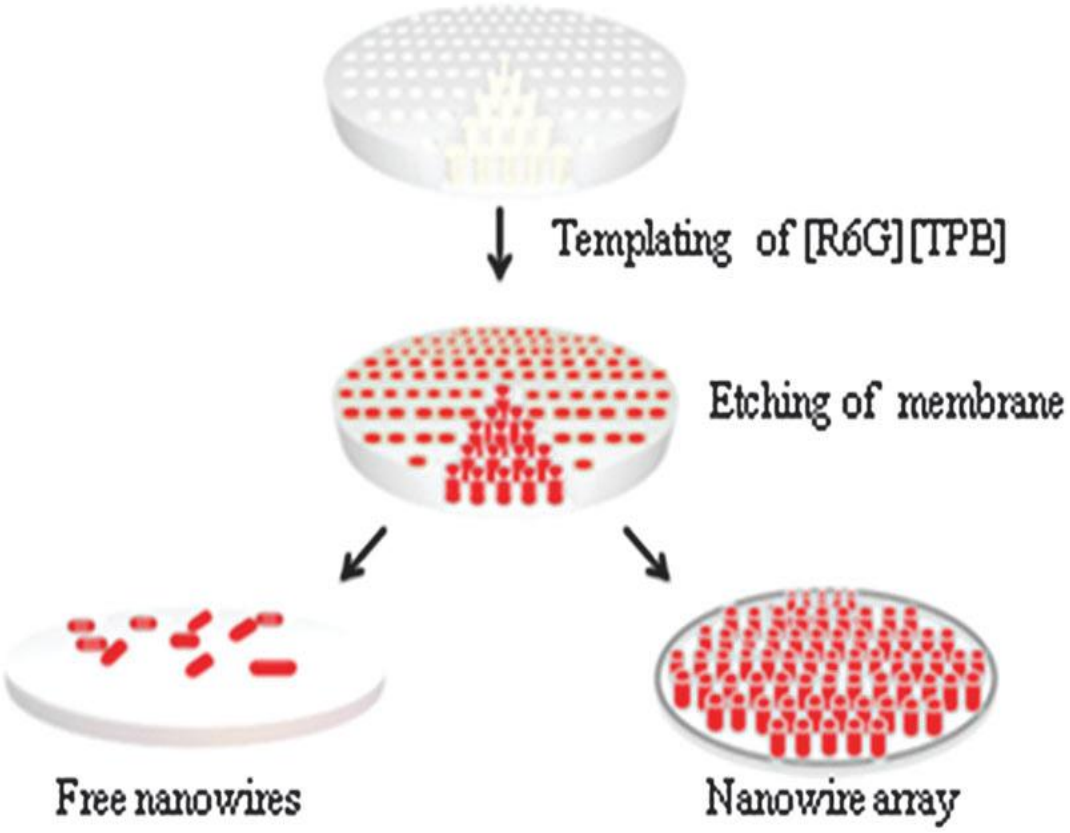

Figure 2.2: Preparation of Nanorods using AAO template. [Appendix A]

2.4 NanoGUMBOS Candidates for Electrical Characterization

In this work, we have used five different types of NanoGUMBOS which differ in chemical composition, morphology and size. In this section, the chemical composition and morphology of each type of NanoGUMBOS is discussed.

1. Rhodamine 6G tetraphenylborate (R6G [TPB])

Figure 2.3 shows the chemical structure of Rhodamine6G tetraphenylborate (R6G [TPB]). This florescent compound is prepared using the anion exchange procedure. The nanowires formed from this material have an average length of 10μm (Figure 2.4 (a)). These nanowires can also be aligned in the form of an array (Figure 2.4(b)) using the *template method* (discussed in section 2.3.1).

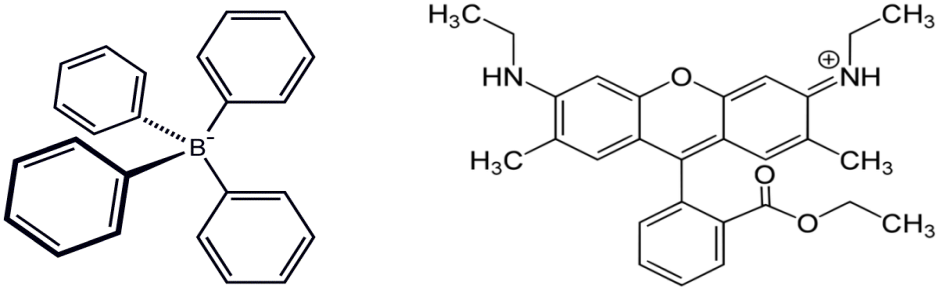

Figure 2.3: Anion (left) and Cation (right) of R6G[TPB] molecule. [Appendix A]

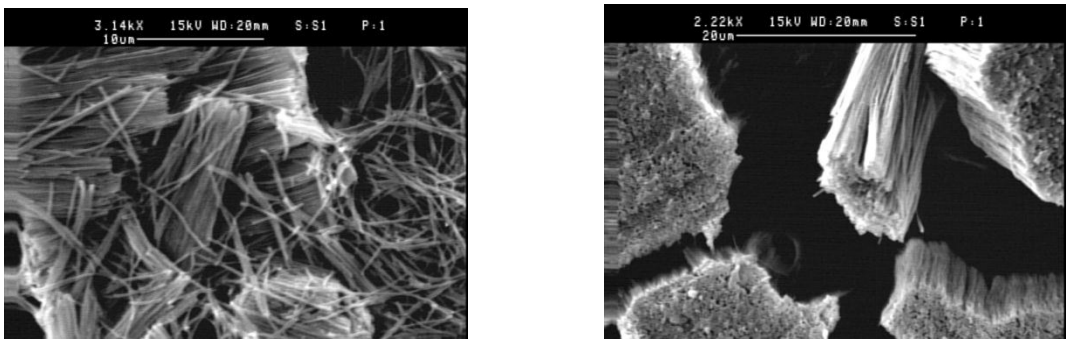

Figure 2.4: SEM images of R6G [TPB] nanowires (a) scattered (b) in the form of an array. [Appendix A]

2. Dimethylpyrollidinium bistrifluoromethanesulfonimide ($Py_{11}Tf_2N$)

The chemical structure of Dimethylpyrollidinium bistrifluoromethanesulfonimide ($Py_{11}Tf_2N$) is shown in the Figure 2.5. Like R6G[TPB], this compound is synthesized using an anion exchange method, and subsequently the template method is employed to make the nanowires.

Figure 2.5: Chemical structure of Py11Tf2N. [Appendix A]

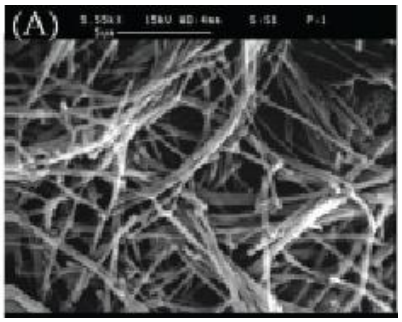

Figure 2.6: SEM image of $Py_{11}Tf_2N$ nanowires. [Appendix A]

3. Pseudoisocyanine bistrifluoromethanesulfonamide ($PIC[NTF_2]$)

The anion exchange method is used to prepare $PIC[NTF_2]$. The *reprecipitation* method is used to make nanoparticles from this compound. This fluorescent compound has a melting point in the range 243°C-248°C and is insoluble in water.

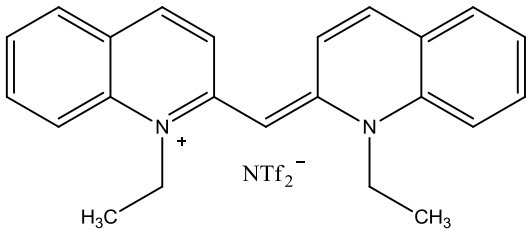

Figure 2.7: Chemical structure of $PIC[NTF_2]$. [Appendix A]

The nanoparticles formed by this compound are diamond shaped as seen in Figure 2.8. The cations in this compound stack into H-aggregates, which in turn explains the morphology of this type of NanoGUMBOS. [40] The particles have an average length of 656 ± 139, a width of 334 ± 74 nm, and a height of 66 ± 30 nm.

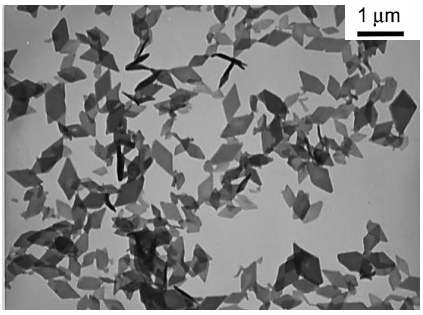

Figure 2.8: TEM image of PIC[NTF_2] diamond shaped nanoparticles. [Appendix A]

4. Pseudoisocyanine bis(perfluoroethylsulfonyl)imide (PIC[BETI])

The anion and cation structure of PIC[BETI] is shown in Figure 2.9. Similar to PIC [NTF_2], this compound is prepared using *reprecipitation*, and the nanowires formed are rod shaped as shown in the Figure 2.10.

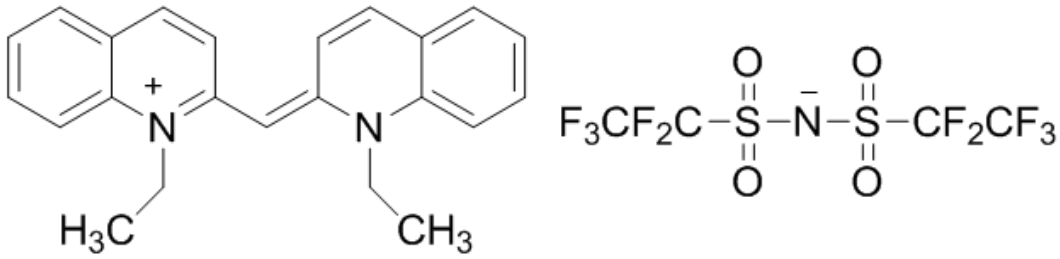

Figure 2.9: Chemical structure of PIC[BETI]. [Appendix A]

The rod shape of nanoparticles formed from this compound is due to stacking of cations into J-aggregates. [40] These nanoparticles have average respective length and width of 1.5 ± 0.83 µm and 88 ± 26 nm, respectively (Figure 2.10).

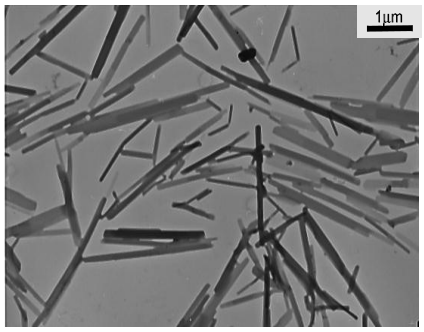

Figure 2.10: SEM image of PIC[BETI] nanorods. [Appendix A]

5. PicopropylSH tetraphenylborate (ProMPyrSH[TPB])

Figure 2.11 shows the chemical structure of ProMPyrSH[TPB], and an SEM image of nanorods formed from the same compound is shown in Figure 2.12. ProMPyrSH[TPB] is synthesized using the anion exchange method, and then nanorods are formed using the template method (discussed in the section 2.3.1).

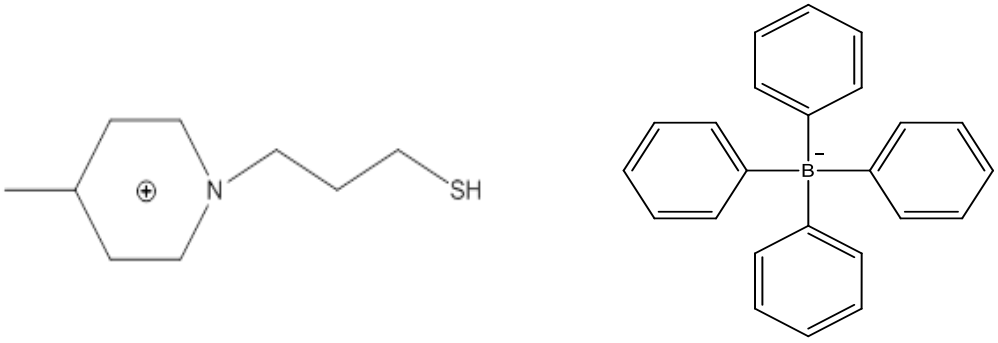

Figure 2.11: Chemical structure of ProMPyrSH[TPB]. [Appendix A]

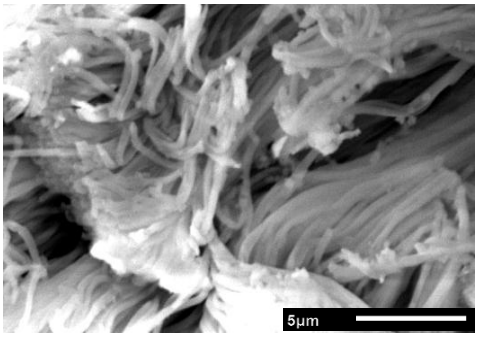

Figure 2.12: SEM image of ProMPyrSH[TPB] nanorods before coating with gold. [Appendix A]

We have used ProMPyrSH[TPB] nanorods as HEMs for electrical and optical characterization. The procedure of gold coating on the nanorods is discussed below—

The AAO disc containing ProMPyrSH[TPB] rods is immersed in 5 mL of 5 nm Au seeds for 48 hours. The Au seeds were flushed using a flow of deionized water. About 5 mL of Au hydroxide solution was then added to the Au-seeded rods, followed by the addition of 25 µL of formaldehyde. After 1 hour, the solution is flushed with deionized water leaving about 5 mL of water remaining. The remaining water was then removed under vacuum. Figure 2.13 illustrates the process of gold coating on ProMPyrSH[TPB] nanorods.

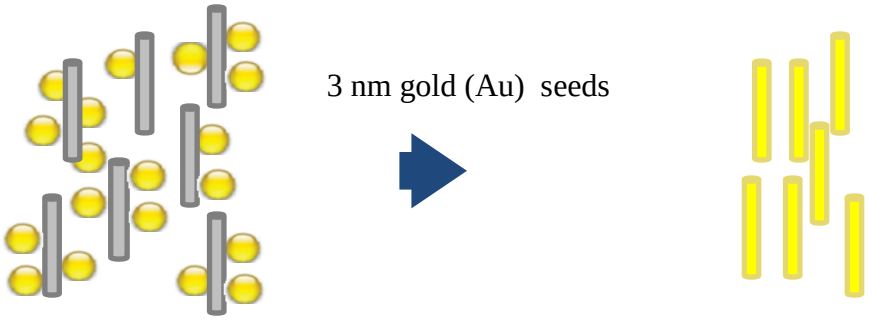

Figure 2.13: Seeding and reduction process of Au on nanorod surfaces. [Appendix A]

2.5 Summary

In this chapter, we have discussed the procedures involved in producing nanoparticles from an ionic liquid (IL). It is important to understand the chemical composition and structure of different species of NanoGUMBOS mainly because the electrical characteristics of NanoGUMBOS vary with respect to chemical composition, specifically changes in cation-anion selection and combinations. The spectral and morphological properties of NanoGUMBOS can be attributed to differences in molecular self-assembly ordering and aggregation. We have also briefly reviewed the preparation steps involved in the formation of gold-coated nanorods, which is a prime candidate for integration into future hybrid electronic device (HED) structures.

3. ATOMIC FORCE MICROSCOPY CHARACTERIZATION OF NANOGUMBOS

3.1 Introduction to Atomic Force Microscopy

Atomic Force Microscopy (AFM) was invented by Gerd Binnig and C.F Quate in 1986. [18] The AFM has its origin in the stylus profiler and the Scanning Tunneling Microscope (STM). With AFM, it is possible to obtain very high resolution images in the nanometer scale. AFM has also enabled measurement, modification and manipulation at the nanometer scale and hence has made a significant impact on the field of Nanotechnology. [19]

The stylus profiler, invented by Schmalz in 1929, utilized an optical lever arm to monitor the motion of a sharp probe mounted at the end of a cantilever. A magnified profile of the surface was generated by recording the motion of the stylus on photographic paper. [19] In 1971, Russell Young demonstrated a non-contact type of stylus profile called the topographiner which used the principle of electronic field emissions between a sharp metal probe and electrically conductive samples. [41] In 1981, researchers at IBM, namely Binning and Heinrich Roher, utilized the methods demonstrated by Young to build a Scanning Tunneling Microscope (STM). [13] They demonstrated that by monitoring electron tunneling currents between the sharp probe and the surface it is possible to see individual atoms on that surface. The STM had limited applications because it worked only on electrically conductive samples.

In 1986, Binnig and Quate demonstrated an advanced version of profilers called the Atomic Force Microscope. [18] Similar to the technique first used by Schmalz, an ultra-small probe tip at the end of the cantilever was used while its motion is monitored by a light-lever sensor. It was possible to achieve high resolutions images using AFM. The theory of operation and different modes of operation of AFM are discussed in detail in this section.

3.1.1 Theory of Operation

The mechanics of AFM is similar to profilers. In AFM, a sharp tip (about 10nm to 40nm radius) is mounted on a cantilever is used. The tip is scanned over a surface with laser beam incident on the head of the cantilever. Figure 3.1 illustrates this configuration. As the tip moves close to the surface, it interacts with the surface forces (e.g. Van der Waals forces). [42] The tip oscillates as it interacts with the surface, and the reflected light intensity varies accordingly. This variation in the reflected light is captured by the detector and then converted to an image.

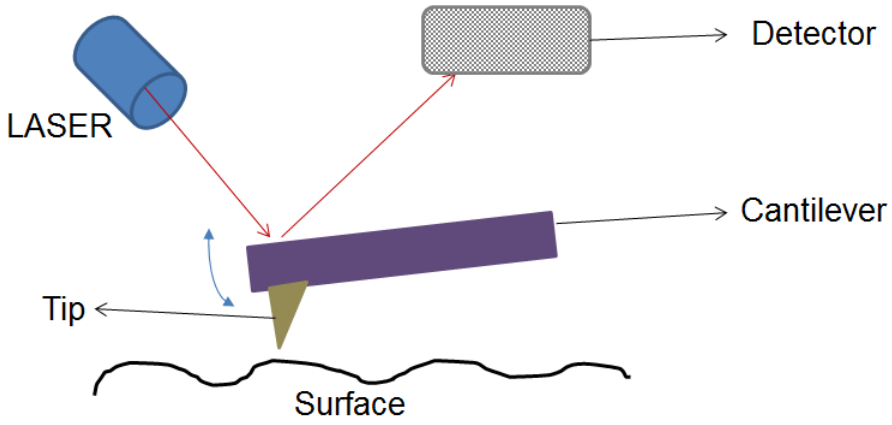

Figure 3.1: Representation of mechanism of AFM.

The AFM is typically operated in two different modes namely – *Contact mode* and *Non-contact mode* (also called 'tapping mode') mode. In contact mode, the tip is in contact with the surface during the scanning process. This mode is generally used in electrical measurements. In the case of non-contact mode, the tip is scanned close to the surface. The tip is oscillated at a certain frequency during scanning. While scanning, the frequency of tip oscillations is affected by the surface forces, and this change in frequency is measured for developing an image. Non-contact mode is ideally used for non-destructive imaging (to avoid surface damage to the tip).

The main components of the AFM are the controller, the AFM stage with probe, the video microscope monitor and a master computer as shown in Figure 3.2. [41]

- The controller has most of the electronics that are required for operating the AFM stage.
- A connection is established between the master computer and the controller. Software programs are used to measure, visualize and analyze AFM images.
- The AFM stage consists of the sample holder, video optical microscope and the scanner. The scanner has the laser, detector and AFM probe holder.
- A monitor connected to the video optical microscope displays the image of probe and the sample.

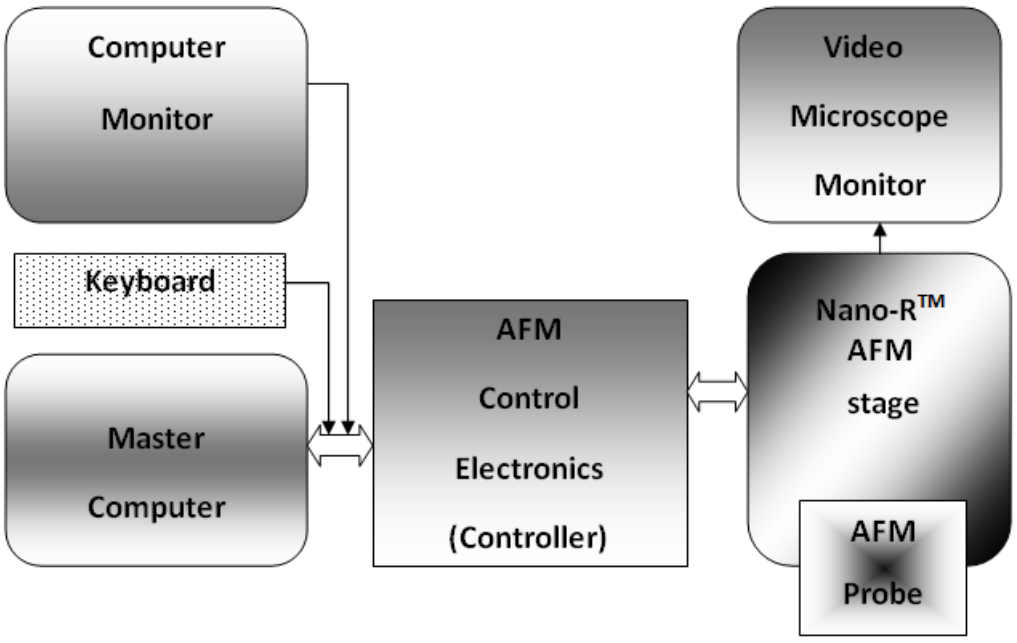

Figure 3.2: Block diagram of the Nano-R™ AFM showing the main components.

3.2 Conductive Probe Atomic Force Microscopy

Using AFM it is not only possible to get the topographical images of samples but also resistance, surface potential, conductance and capacitance. For example, a conductive tip can be

used to electrically characterize the sample surface based on the dynamic electric forces. Figure 3.3 shows the schematic representation of conductive probe AFM (CP-AFM).

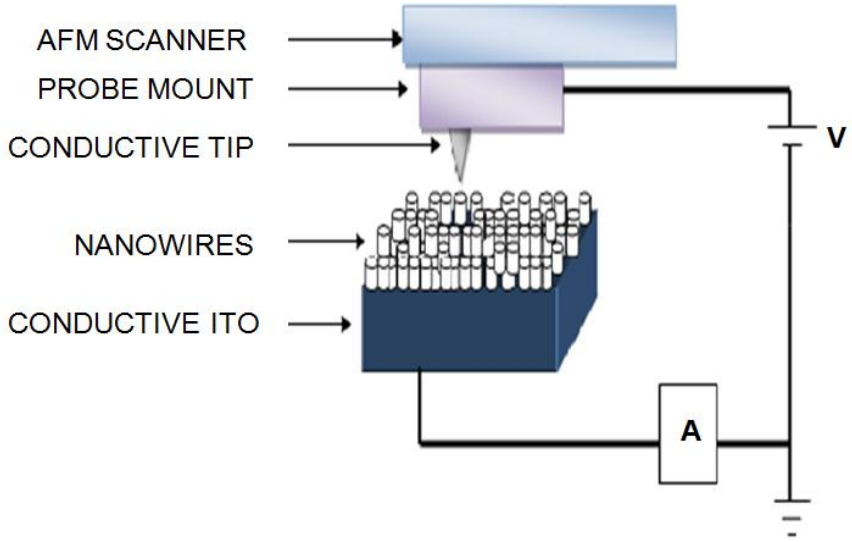

Figure 3.3: Representation of Conductive probe AFM (CP-AFM).

3.2.1 CP-AFM Experimental Setup

A Pacific Nanotechnology (now Agilent) atomic force microscope (AFM) with a conductive tip (silicon coated with platinum) was operated in *Contact mode*. The tip was used as one of the electrodes with the other being the sample base (conductive Indium Tin Oxide (ITO) or a gold surface) as shown in Figure 3.3. A closed circuit is formed when the tip is in contact with the sample, which may be nanoparticles or nanowires.

The advantage of using CP-AFM is that both electrical properties and topography can be obtained simultaneously which helps in placing the tip on the structure to be measured. In our work, the AFM tip was placed on the open end of a nanowire. The voltage was swept from -1V to +1V, and current was measured using a Keithley Semiconductor Characterization System (SCS). Resistivity and conductivity were deduced using the dimensions of nanowires which were

determined by Pacific Nanotechnology-NanoRule™ AFM imaging software. Figure 3.4 is a set of schematically defined photographs of our CP-AFM setup.

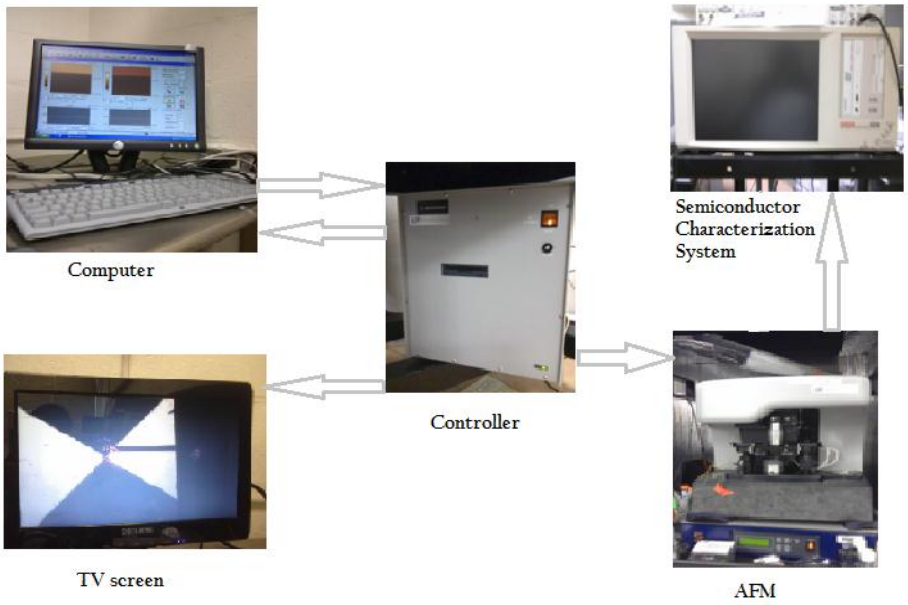

Figure 3.4: Schematic representation of CP-AFM setup.

The most common reason for using a conductive tip for electrical measurements is that the contact area is minimized with surface objects such as nanoparticles/nanowires, which in turn reduce the contact resistance.

3.3 Results of CP-AFM Measurements on NanoGUMBOS

The AFM images of five types of NanoGUMBOS were obtained prior to current-voltage measurements. For imaging purpose, the AFM was operated in contact mode with an n-type silicon probe from Mikromasch. Pacific Nanotechnology-NanoRule software was used to obtain the surface as well as 3D images of all the samples. Current-Voltage (I-V) measurements on all the types of NanoGUMBOS were done using the CP-AFM method.

Figure 3.5 shows the 3D image (with scan area of 40μm x 40μm) of an array of Rhodamine6G tetraphenylborate (R6G[TPB]) nanowires standing on Indium Tin Oxide (ITO). The nanowires were prepared by the Warner Group using anion exchange method followed by

template method (preparation is explained in chapter 2). [39] The color scale on the right hand side of the image gives the maximum and minimum heights of the surface features. The image shows nanoscale structures with different heights ranging from 5000 nm to 10,000 nm (5μm to 10μm). The AFM image also shows abrupt variations that are mainly due to image artifacts that occur during the scanning process. The image artifacts occur when the probe diameter is larger diameter than the feature size or if there is error in the orthogonality of the motion of the scanner or scan rate. [19]

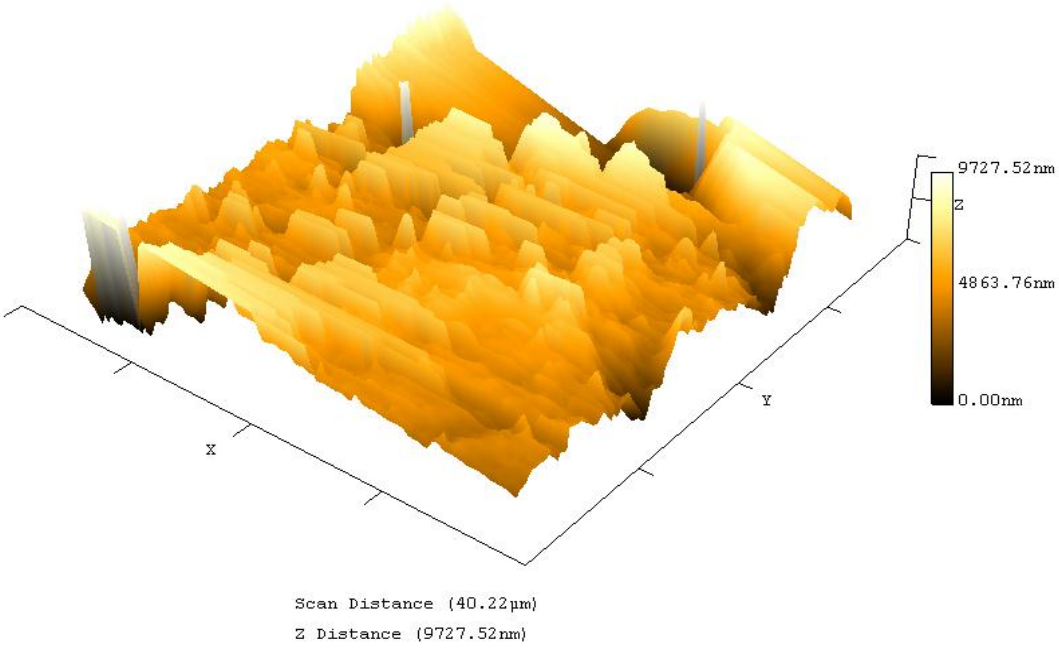

Figure 3.5: AFM 3D image of R6G[TPB] nanowire array

I-V measurement on R6G[TPB] nanowires using the CP-AFM method is shown in Figure 3.6. The voltage was swept from -1V to +1V, and the measured curve shows nearly symmetric and linear behavior. The resistance of this nanomaterial was found to be approximately 35MΩ. We verified this result with I-V curves obtained using a "drop cast" method also developed in

our group to measure the current through the nanowires.[1] This method involves a more conventional approach in which nanowires are placed between interdigitated fingers (IDF) of gold to obtain the electrical measurements (Figure 3.7 (a)). The order of current observed in CP-AFM is in close correlation with that of I-V obtained using the IDF method (Figure 3.7 (b)).

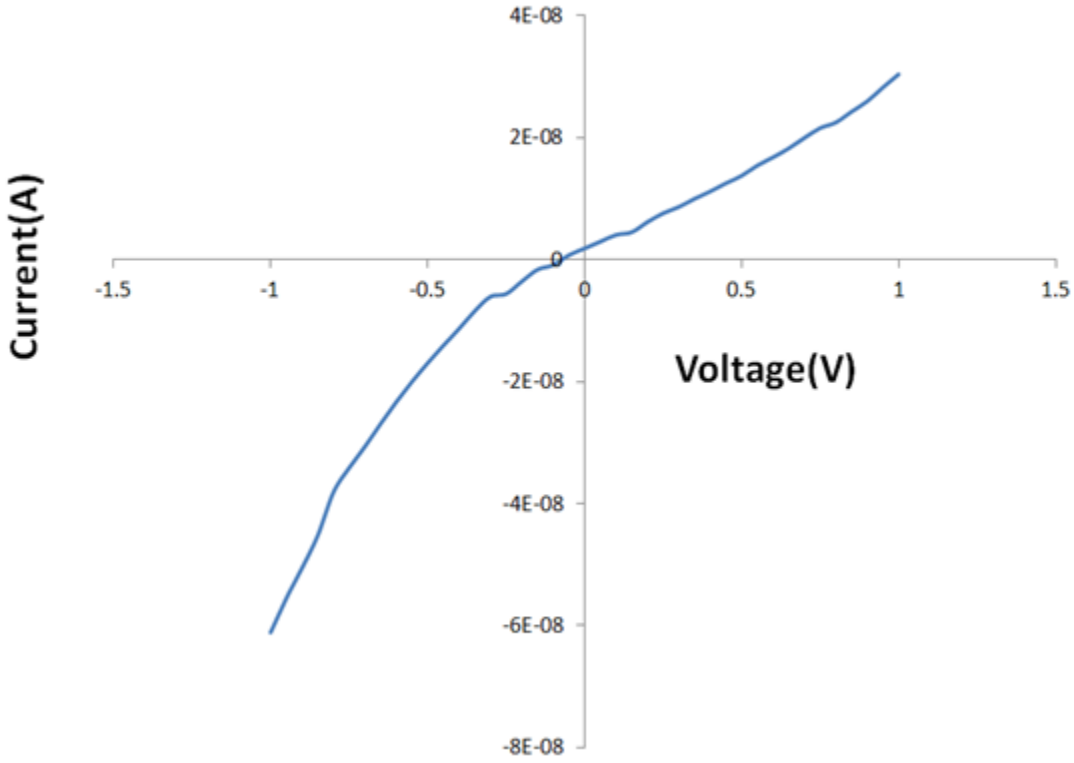

Figure 3.6: I-V of [R6G] [TPB] on gold plated mica using CP-AFM .

[1] Drop cast technique involves placing the nanowires (in a solution) between two conducting gold structures that are separated by a small insulating gap. The solution is allowed to dry, leaving behind the nanowires.

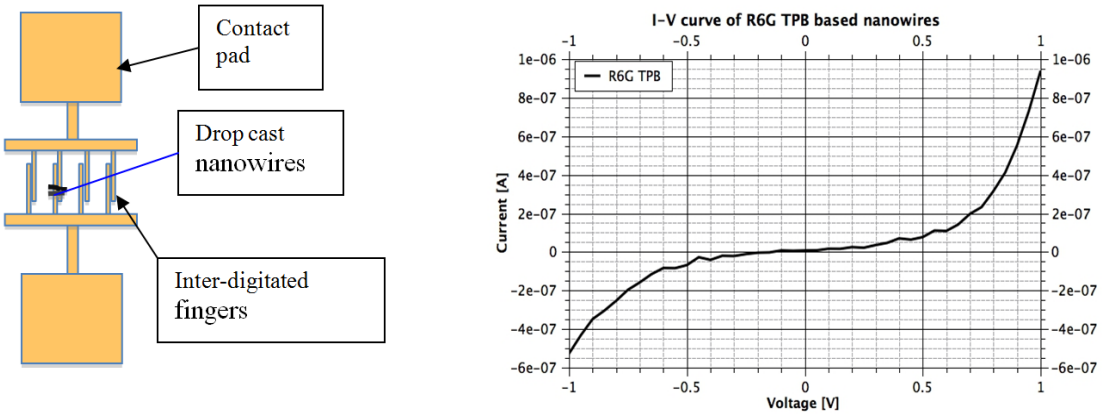

(a) (b)

Figure 3.7: (a) IDF contact pads (b) I-V of R6G [TPB] nanowires measured using IDF contact pads.

Figure 3.8 shows the AFM 3D image of a Dimethylpyrollidinium bistrifluoromethanesulfonimide ($Py_{11}Tf_2N$) nanowire array on ITO glass. These nanowires were prepared using a *template method* (discussed in chapter 2). The spikes that are seen on the blue background are the nanowires. This image was scanned over a surface area of 100µm x 100µm.

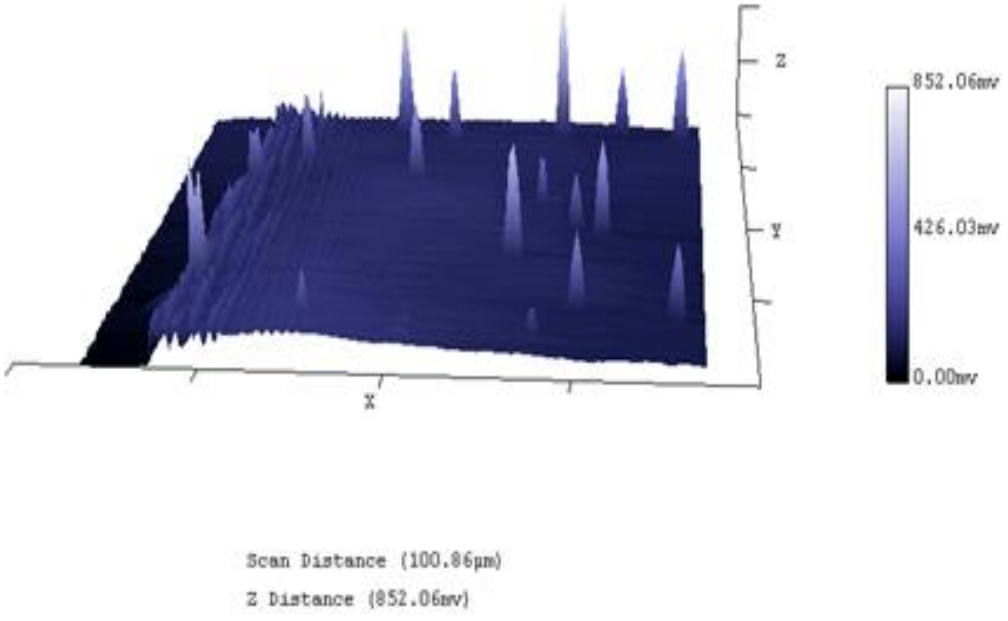

Figure 3.8: AFM 3D image of $Py_{11}Tf_2N$.

I-V plot of $Py_{11}Tf_2N$ is shown in Figure 3.9. The curve shows non-symmetric and non-ohmic behavior similar to that of a p-n junction diode. There is low current observed in the negative voltage region. In the positive voltage regime, the current is almost zero until a certain point and then increases dramatically. A small plunge is observed in the positive regime (at +0.7V). We suspect that this may happen due to oxidation process or decomposition of the compound. [43] The magnitude of current through $Py_{11}Tf_2N$ is one order lower than the R6G [TPB] nanowires. The resistance was measured by selecting the ohmic region in the plot, and it was calculated to be around 280MΩ.

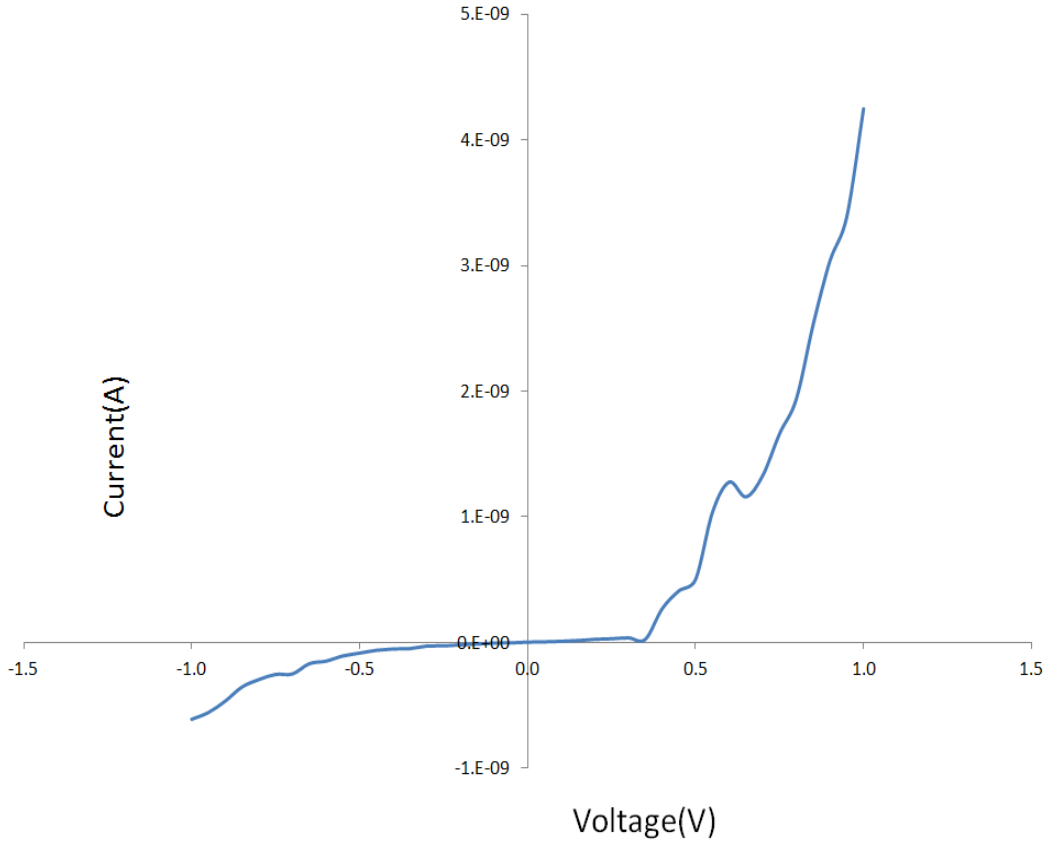

Figure 3.9: I-V of $Py_{11}Tf_2N$ on gold plated mica using CP-AFM.

The third type of NanoGUMBOS that we have used for electrical measurements is Pseudoisocyanine bistrifluoromethanesulfonamide (PIC[NTF_2]). These fluorescent nanoparticles were prepared by a *reprecipitation* method. [40] For imaging purposes, these nanoparticles were placed on a gold surface using again our drop cast method. Figure 3.10 (a) & (b) show the AFM images of diamond shaped structures similar to the TEM image (discussed in Chapter 2). These nanoparticles have width ranging from 0.5µm to 1µm and average height is about 60nm.

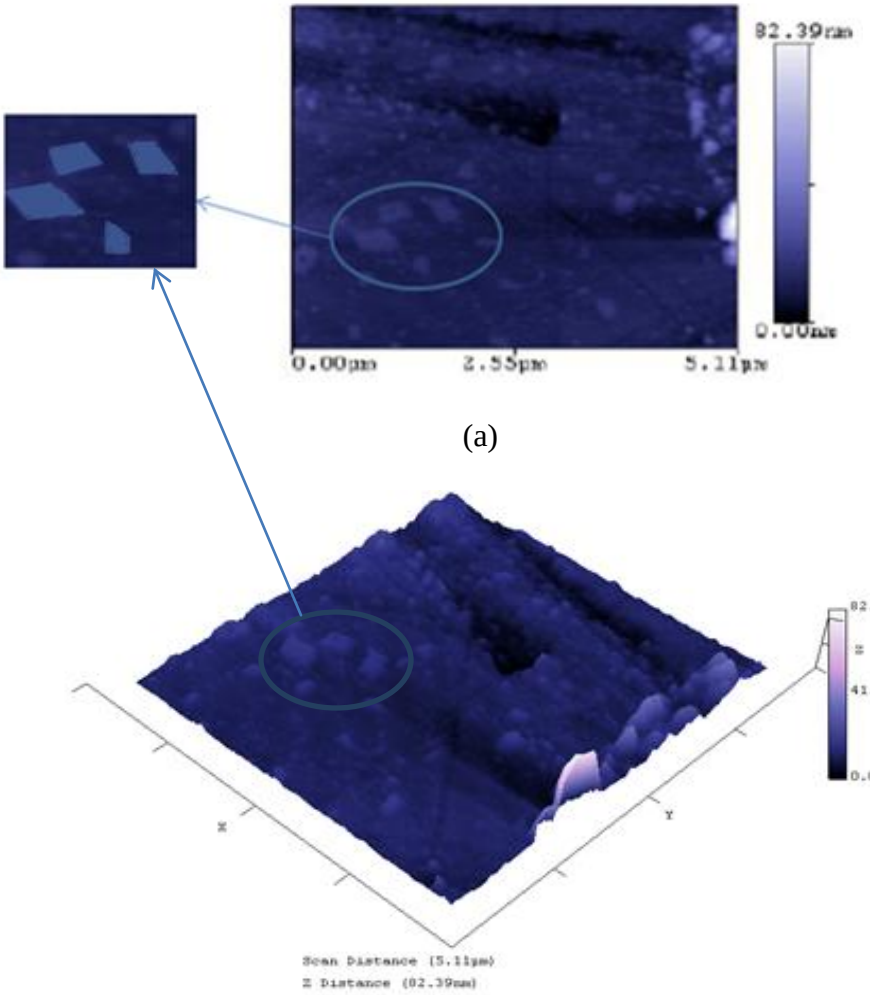

Figure 3.10: (a) AFM surface topography of PIC[NTF_2] nanoparticles dried on gold-coated mica and (b) AFM 3D image

Figure 3.11 shows symmetric I-V behavior of PIC[NTF_2] measured using CP-AFM. The voltage was swept from -2V to +1V in order to correlate the current behavior with oxidation/reduction process of the material in liquid state. The dip seen in the positive voltage regime (around +0.3V) could be due to oxidation within the nanoparticle. The order of magnitude of current lies below the range observed in $Py_{11}Tf_2N$. The I-V curve shows an exponential rise in current with respect to voltage. The ohmic resistance of this type of NanoGUMBOS was found to be 30GΩ.

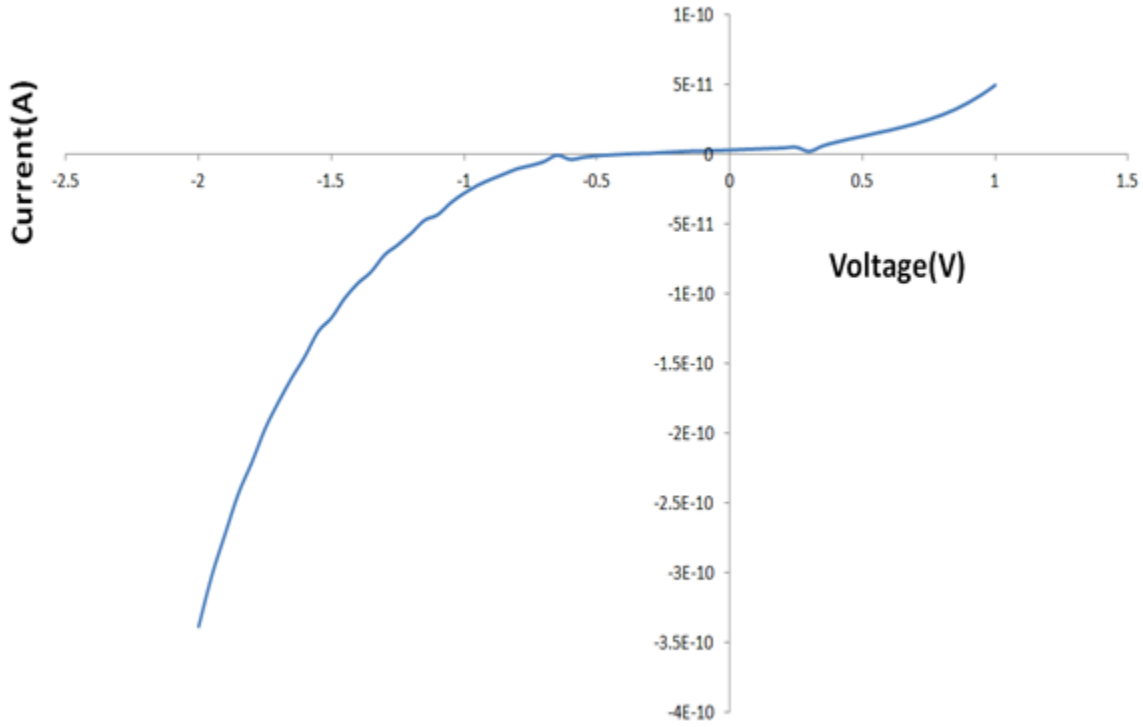

Figure 3.11: Current-voltage data on PIC[NTF_2] on gold plated mica using CP-AFM.

The fourth type of NanoGUMBOS that we have electrically characterized is Pseudoisocyanine bis(perfluoroethylsulfonyl)imide PIC[BETI]. Similar to PIC[NTF_2] nanoparticles, these fluorescent nanoparticles are prepared by a *reprecipitation* method. [40] Figure 3.12 shows the AFM surface topography of PIC[BETI] nanorods. This species of NanoGUMBOS was drop cast on a smooth gold-coated mica surface for imaging purpose. The length, width and height of these nanorods were found to be ~1μm, ~360nm and ~300nm, respectively.

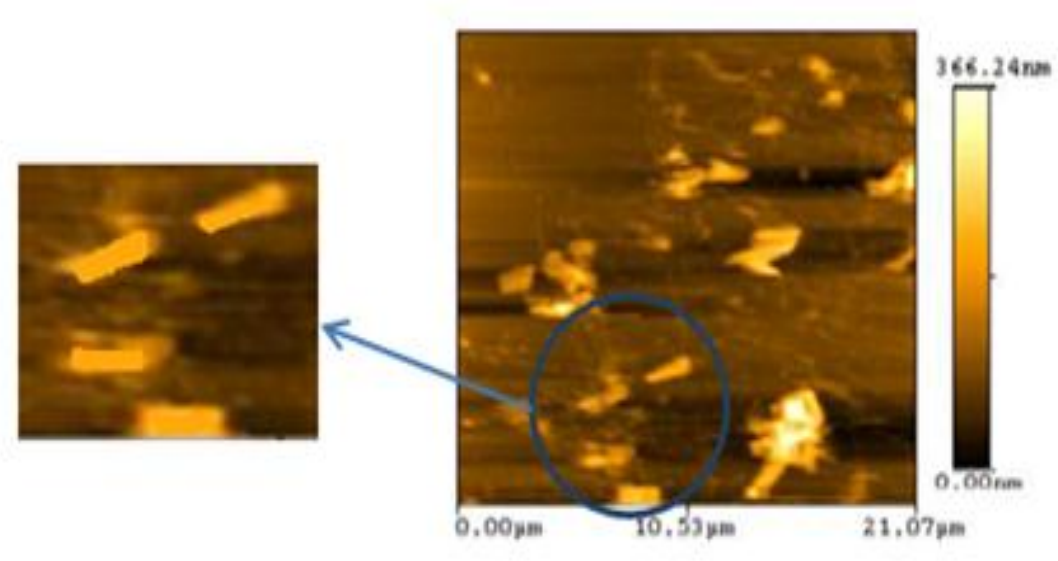

Figure 3.9: AFM topography of PIC[BETI] nanorods on gold surface.

I-V characteristics of PIC[BETI] nanorods (Figure 3.10) show exponential behavior similar to PIC[NTF_2]. Again, we speculate that the current plunges (at -1.7V and +0.6V), which are seen in both positive and negative regimes, could be because of oxidation process within the material. The average resistance of this type of NanoGUMBOS was found to be 385GΩ.

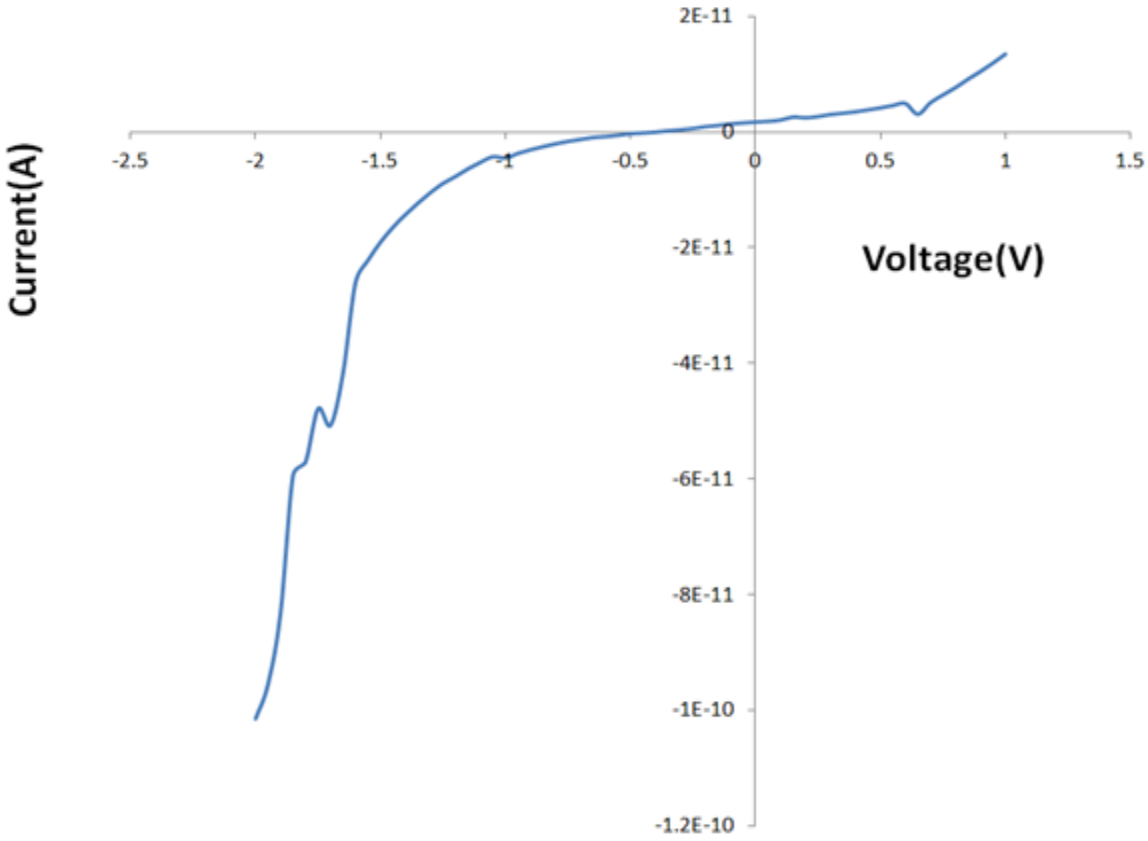

Figure 3.10: I-V of PIC[BETI] on gold-coated mica using CP-AFM.

Figure 3.11 shows AFM topography of PicopropylSH tetraphenylborate (ProMPyrSH[TPB]) nanorods. Theses nanorods were prepared using an anion exchange method. [39] We have used this type of NanoGUMBOS for HEMs purposes by combing them with gold. The AFM imaging was done before coating the nanorods with gold. The average length of the nanorods was found to be 500nm.

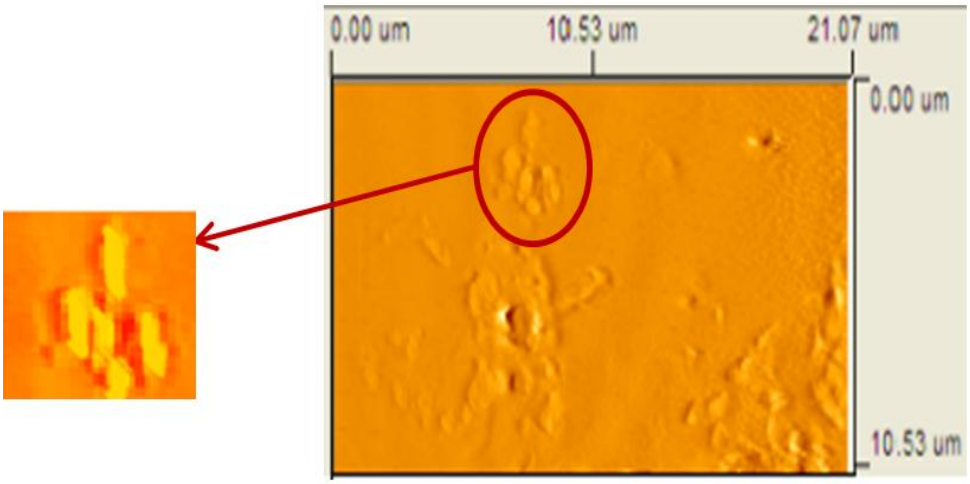

Figure 3.11: AFM topography of ProMPyrSH[TPB] nanorods on gold surface.

By combining NanoGUMBOS with substrates of more traditional materials, such as metals or semiconductors, these nanoscale particles could serve as HEMs. For example, by coating the NanoGUMBOS with gold a 'metal-NanoGUMBOS-metal' junction is formed. The current-voltage curves of both bare nanoparticles and gold coated nanoparticles were measured. Significant rise in the current was observed with the latter sample. The following plots (Figure 3.12 show the difference in current before and after coating the nanoparticles with gold.

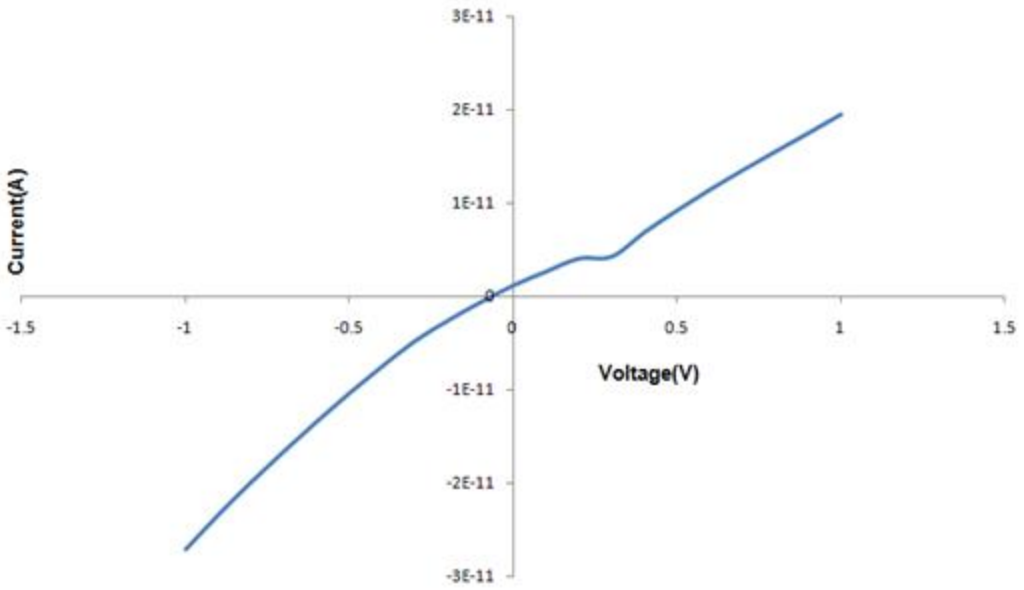

Figure 3.12: I-V of ProMPyrSH[TPB] nanorods on gold-coated mica using CP-AFM.

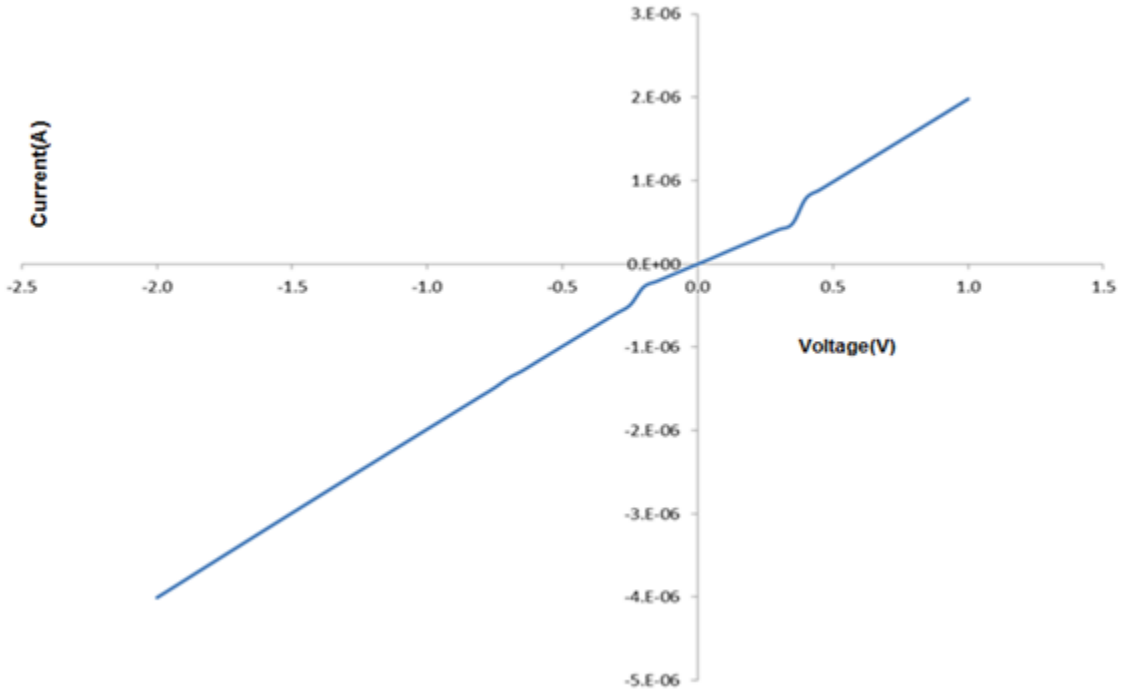

Figure 3.13: Increase in current observed after coating the nanoparticles with gold.

3.5 Summary

We have observed conductivity in this new material. The mechanism and advantages of conductive probe AFM has been discussed. We have successfully measured current vs. voltage (I-V) characteristics of different types of NanoGUMBOS using conductive probe-AFM. We have studied the morphology and current behavior of each type of NanoGUMBOS in solid form and also made an attempt to correlate them with the chemical reactions that are observed in the liquid state of the material. Dimensions of nanoparticles were determined using the AFM topographies. Other electrical properties like resistivity and conductivity can be deduced using the dimensions and I-V plots.

4. RAMAN SPECTROSCOPY OF NANOGUMBOS

4.1 Introduction to Raman Spectroscopy:

In 1928, Professor C.V Raman demonstrated a vibrational spectroscopy technique for which he was awarded the Nobel prize in Physics in 1930. This technique involves the study of monochromatic light (from a laser) as scattered by a sample. The frequency of the incident photons is altered upon interaction with the surface molecules resulting in inelastic scattering which, by definition, occurs when the scattered photon has a higher or lower frequency compared to the original monochromatic frequency. [44] This phenomenon is called the "Raman effect," and the analysis of photons arising from the Raman effect is called "Raman Spectroscopy."

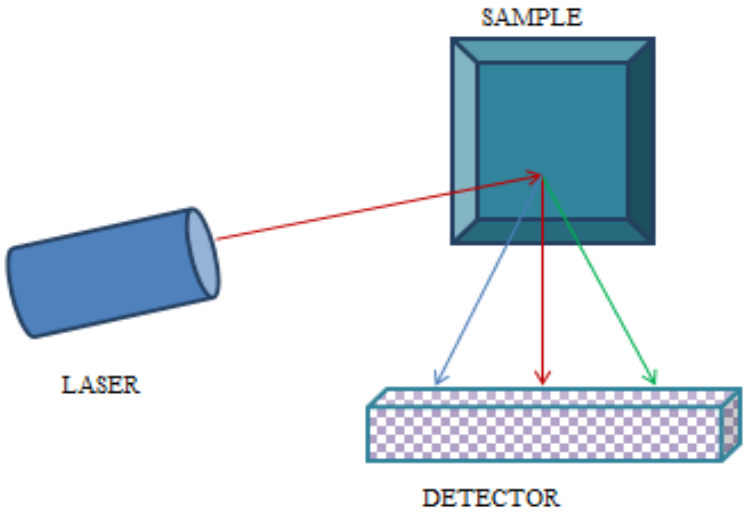

Figure 4.1: Schematic of Raman scattering

The change in frequency of the scattered photon provides chemical and structural information on a sample under investigation. Hence, Raman spectroscopy can be used to determine the chemical structure, vibrational state and orientation of molecules as well as effects of bonding, environment and stress on a sample.

Light scattered from a molecule has mainly three components as follows (Figure 4.2):

1. Stokes Raman scattering: In this type of scattering, the wavelength of photons reflected from the molecule is longer than the wavelength of the incident photon. The difference in wavelength is due to absorption of energy by the molecule in the lower vibration level.

2. Rayleigh scattering: This type of scattering involves the reflection of photons having the same wavelength as that of the incident photon. There is no loss or gain of photon energy during the process.

3. Anti-Stokes Raman scattering: This occurs when photons are reflected from a molecule in the higher vibrational state. The photon gains energy upon collision with the molecule and thereby scatters with a wavelength shorter than the incident light.

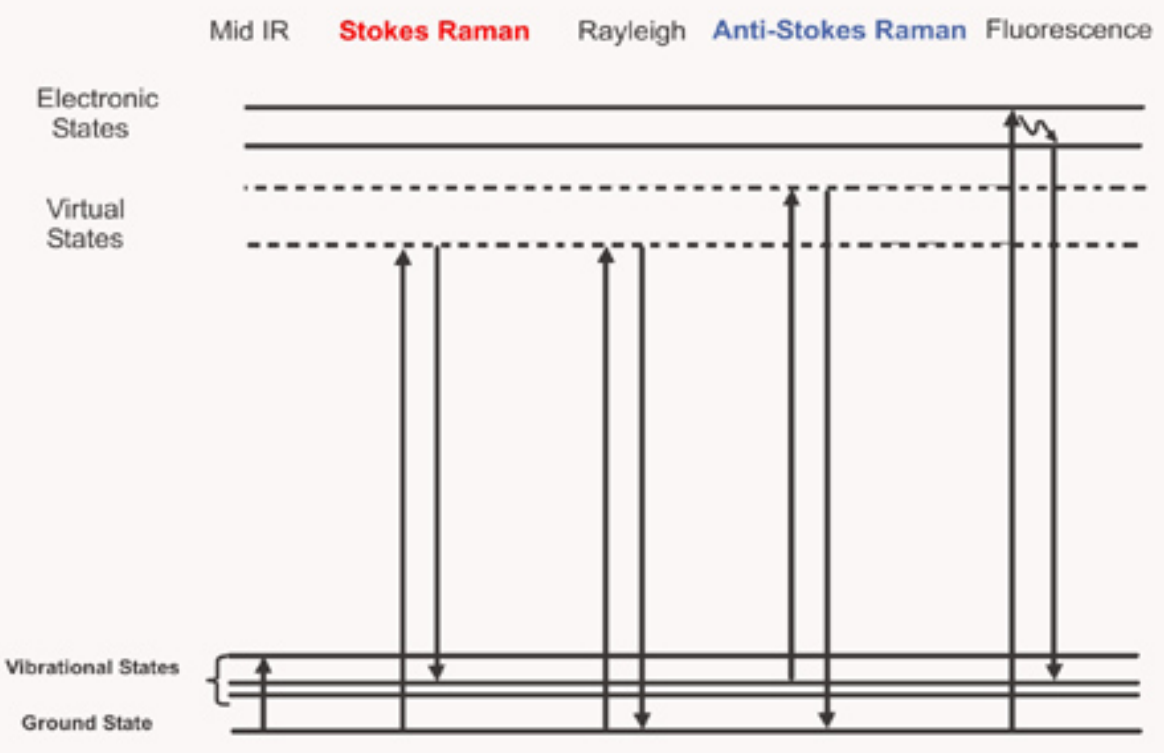

Figure 4.2: Illustration of scattering processes. [45]

4.1.1 Polarizability and Raman Shift:

When light with electric field strength (E) falls on a diatomic molecule, an electric dipole moment (P) is induced given by:

$$P = \alpha E \quad (4.1)$$

where α is a proportionality constant and is called polarizability.

Raman shift is defined as the difference in the wavenumbers between the laser (source) and the scattered photons, and it is represented by the following equation:

$$\Delta\nu_{\text{Raman shift}} = \nu_{\text{Laser}} - \nu_{\text{Scattered}} \quad (4.2)$$

The intensity of the Raman scattering depends on the number of molecules being excited in the sample. A shift in the wavenumber (cm^{-1}) depends on the chemical structure of the molecule upon which the photons are incident.

4.1.2 Raman Instrumentation:

A Raman Spectrometer consists of the following basic parts [45]:

1. Excitation Source (usually a laser).
2. White light source and optical microscope to focus the sample.
3. Wavelength selector (Filter or Spectrophotometer).
4. Detector (CCD or Photo diode array).

The process of Raman spectroscopy is shown in the figure (4.3). First, the sample is illuminated with white light. Using the video optical microscope the lens is positioned above the spot of interest. Light from a monochromatic laser source is passed through the optical arrangement consisting of lens and filters and then to the microscope. The scattered light from the sample is captured by the spectrophotometer which selects the wavelength by using a diffraction grating.

The detector which is usually made of a CCD (charge coupled device) records the signal and feeds it to the software that decodes and plots the graph of Intensity vs. Raman shift.

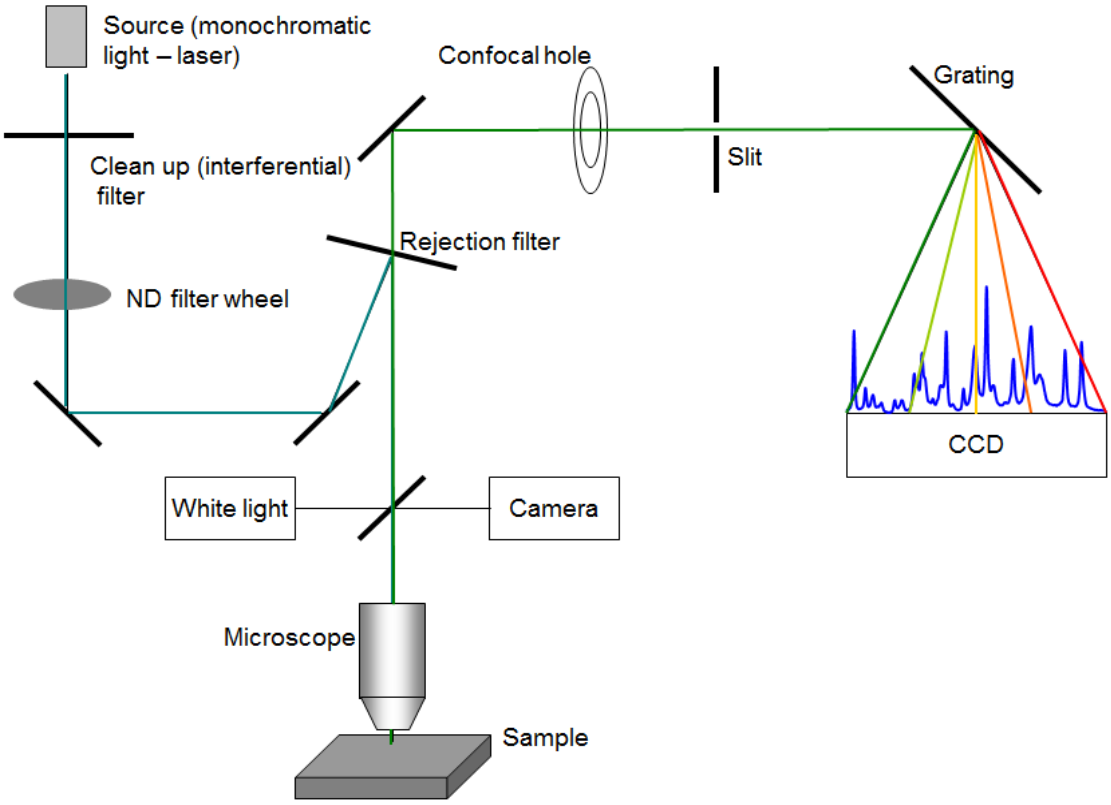

Fig 4.3: Illustration of Raman Spectroscopy technique. [Appendix A].

4.2 Different Techniques to Enhance Raman Scattering:

The intensity of scattered Raman light is very low with respect to incident light in the ratio of $1:10^{-10}$. [45] Therefore, it is necessary to enhance the Raman peaks. There are different techniques to improve the Raman signals like Resonance Raman, Surface Enhanced Raman Spectroscopy (SERS) and Surface Enhanced Resonance Raman Spectroscopy (SERRS).

1. Resonance Raman Spectroscopy: In this technique, a laser source with frequency corresponding to the electronic transition states of a particular molecule is chosen. Under such conditions, the intensity of the Raman bands can be enhanced by a factor of 10^3 to 10^5. [44]

2. Surface Enhanced Raman Spectroscopy (SERS): When molecules are adsorbed on the surface of metals the strength of the Raman spectra increasingly drastically. To explain this phenomenon of surface enhancement two theories have been proposed. Both theories explain the effect using the following equation for dipole moment: $P = \alpha E$

where, α –> Molecular polarizability

E –> Electric Field

The intensity of a Raman signal is directly proportional to the square of the induced dipole moment. So, there should be an increase in the value of either α or E that causes an increase in intensity. The first theory says that, due to laser light field interaction with conduction electrons in metal atoms, a surface plasmon, resonance is generated, and the electromagnetic field (E) increases significantly. The second theory says that charge transfer or bond formation of the metal and adsorbate increases the molecular polarizabilty (α). [45]

3. Surface Enhanced Raman Spectroscopy (SERRS): This technique is a combination of Resonance Raman and SERS techniques. SERRS has proven to be more advantageous than other techniques in terms of the enhancement of Raman signals.

4.3 Comparison of Raman Spectroscopy with Infrared Spectroscopy (IR):

Both Raman and IR spectroscopies are based on vibration of the molecules. Raman spectroscopy has advantages and disadvantages when compared to IR. There are many advantages to Raman Spectroscopy over IR. Some of them are as follows:

1. Totally symmetric vibrations can be seen only through Raman spectroscopy.
2. Some vibrations that are weak in IR can be strong in Raman spectra.

Some disadvantages include local heating and/or photodecomposition of the material, the fluorescence of the material affecting the Raman spectral intensity and the high cost of the system. [44]

Table 4.1: Differences between Raman and IR spectroscopy

Sl.no	**Raman Spectroscopy**	**Infrared Spectroscopy**
1.	Based on scattering.	Based on absorption.
2.	Probes *non-polar* modes.	Probes *polar modes* - modes that modify existing dielectric dipole moments of molecules.
3.	Involves two beams of radiation - illumination and collection. The scattered intensity depends on the orientation of the molecule with respect to the polarization vectors of both beams.	Involves only one beam of polarized radiation. The amount of radiation absorbed by a molecule depends only on the orientation of the molecule with respect to the polarization vector of the radiation.
4.	Little or no sample preparation is required.	In most cases sample preparation is required.

4.4 Applications of Raman Spectroscopy:

In electronics, obtaining the Raman spectral signature of the nanoparticles is advantageous in the following ways:

1. Optical detection or identification of nanoparticles [46] – In this case different types of nanoscale electronic components (differing in the chemical composition and molecular orientation) are placed on the same circuit board, Raman characteristics of each nanomaterial can be used to differentiate and identify them.
2. Raman microscopy – This advancement in Raman application utilizes Raman results from different materials and produces the Raman image of the surface area. This image could be used to analyze the concentration of a particular material on the surface.
3. Stability test - Raman signatures of a nanomaterial can be used to study the stability and change in electrical properties due to variation in physical changes like temperature and current.
4. Raman spectroscopy can also be used to study the effect of impurities and defects in the nanowires.

Raman spectroscopy has become an important analytical and research tool. Other applications include:

- Pharmaceuticals
- Forensic Science
- Polymers
- Thin Films
- Semiconductors
- Material Research – analysis of corrosion

4.5 Raman Spectroscopy of NanoGUMBOS:

Phonon behavior in nanoparticles is different when compared to bulk material. Due to phonon confinement in the nanoparticles, the carrier-phonon interaction is altered. So, understanding confined phonon effects in the nanowires is necessary to analyze the electron-phonon interaction and for device enhancement. Using Raman Spectroscopy we can measure the phonon dispersion and the lifetime of the phonons in nanostructures. [47] If the lattice structure of the organic compound is known, then it is easy to understand the electron flow and interaction with the vibration of molecules. In this work, we have obtained the Raman spectra for different types of NanoGUMBOS and identified the Raman bands results with respect to the chemical structure of the organic molecules.

4.5.1 Experimental Setup:

Raman spectroscopy measurements were obtained using a Horiba Raman spectrometer. The readings were taken with the following setup:

1. The nanoparticles were focused at 50x/100x magnification in the optical microscope.
2. The experiment was conducted at room temperature.
3. Nanoparticles were incorporated into the glass-coated structure as shown below.

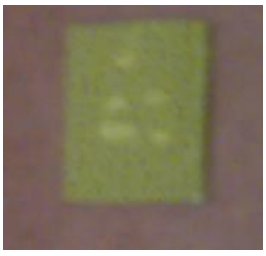

Figure 4.4: Nanoparticles on gold surface by drop coating.

4. Laser with wavelength 638.4nm was incident on the nanoparticles and spectroscopy data was obtained using Labspec software.

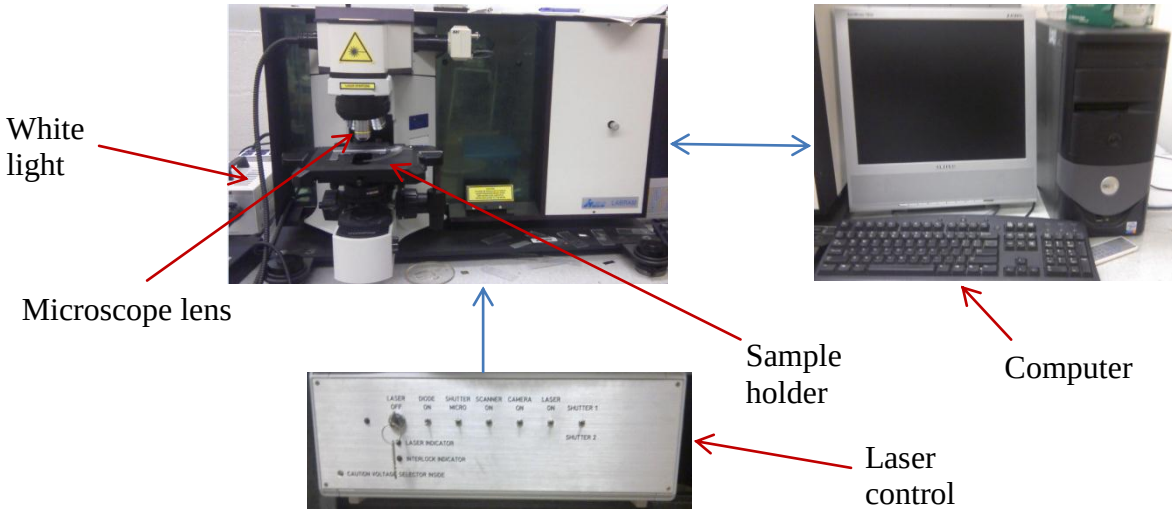

Figure 4.5: Schematic of Raman Spectroscopy Instrumentation

5. Plot of Intensity vs. Raman Shift (cm^{-1}) was obtained indicating the Raman peaks of the nanoparticles.

4.5.2 Results and Analysis:

We have obtained Raman signatures of three types of NanoGUMBOS. The nanoparticles were placed on gold or silicon surface in all our experiments. The Raman peak for atomically smooth silicon is commonly known to be at $521cm^{-1}$. So, this standard value is helpful for making sure that there are no impurities on the surface. The Raman spectra of gold and silicon were obtained before placing the nanoparticles. Figure 4.6 shows the plot of Intensity vs. Raman shift of silicon with peak at $521cm^{-1}$, and Figure 4.7 shows no peaks for gold. In case of NanoGUMBOS, we have correlated the peaks with standard Raman bands and also attempted to identify the chemical bonds responsible for those peaks.

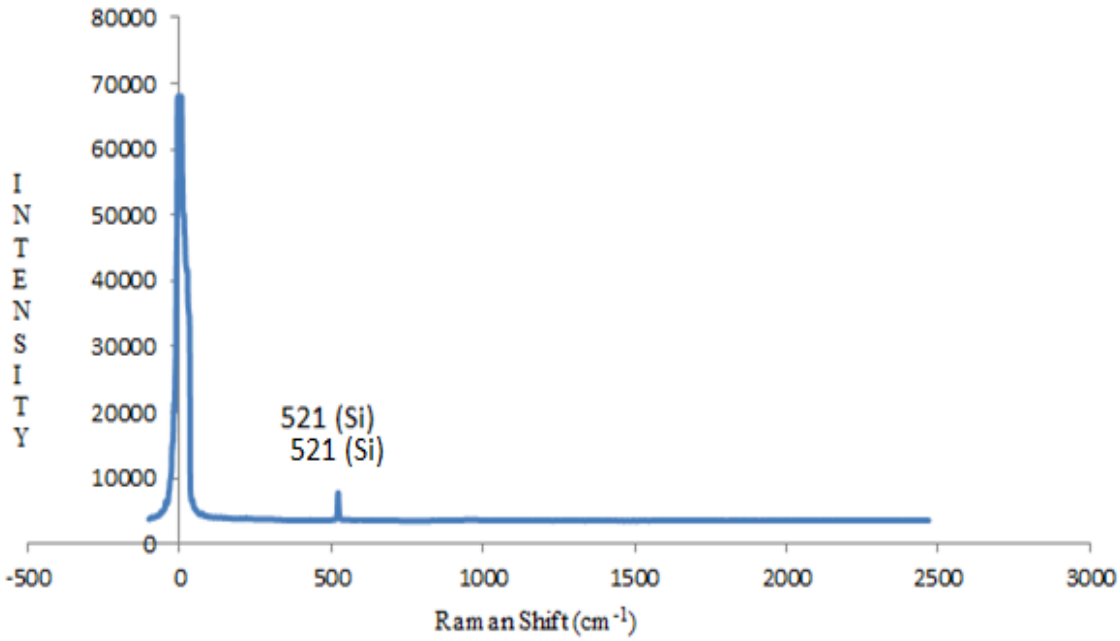

Figure 4.6: Raman spectra of Silicon showing peak at 521 cm^{-1}

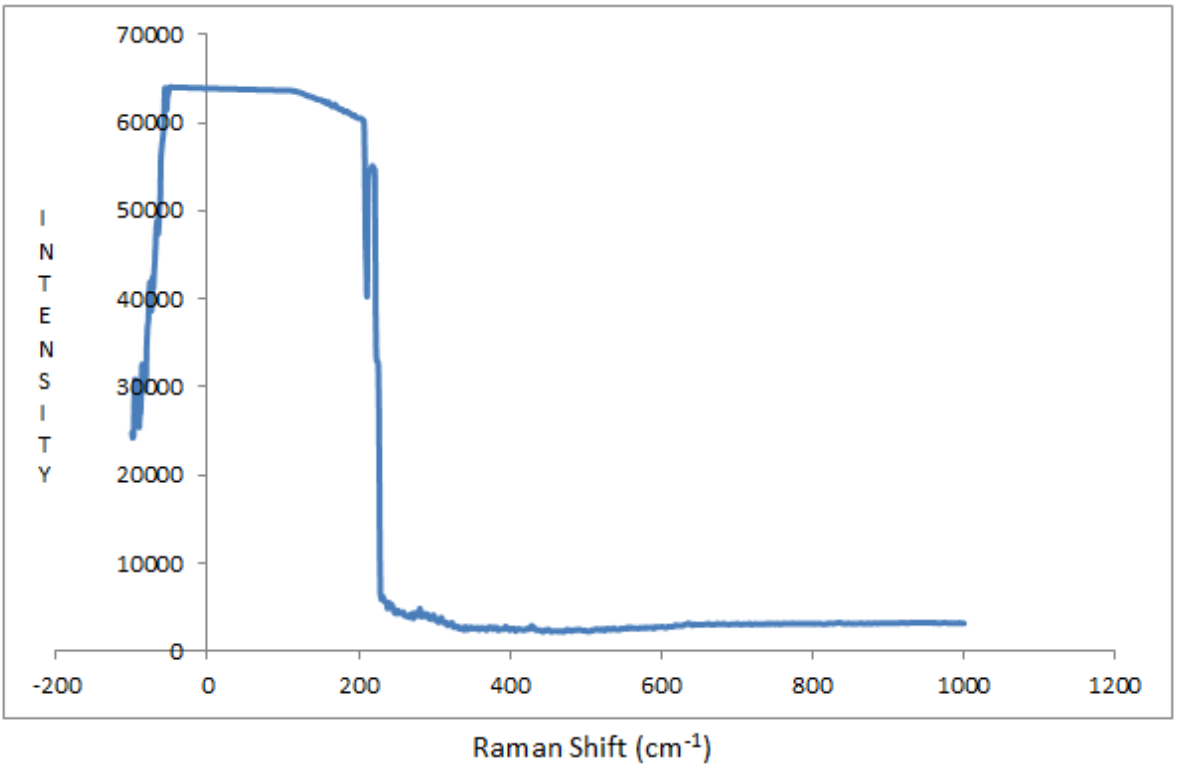

Figure 4.7: Raman spectra of gold showing no peaks.

The first type of NanoGUMBOS that we have used for Raman analysis is Rhodamine6G tetraphenylborate (R6G[TPB]). Figure 4.8 shows Raman spectra of (R6G[TPB]) nanowires (preparation of nanowires is discussed in Chapter 2). The Raman peaks at 614cm^{-1}, 771cm^{-1}, 1183cm^{-1}, 1311cm^{-1}, 1364cm^{-1}, 1510cm^{-1}, 1571cm^{-1} and 1648cm^{-1} are because of the R6G molecule. [48][49] At 833cm^{-1} and 1027cm^{-1}, the bands could not be identified, but they are seen on both silicon and gold surfaces. The rise in the intensity, which is seen in both plots, could be due to the fluorescence effect of the compound.

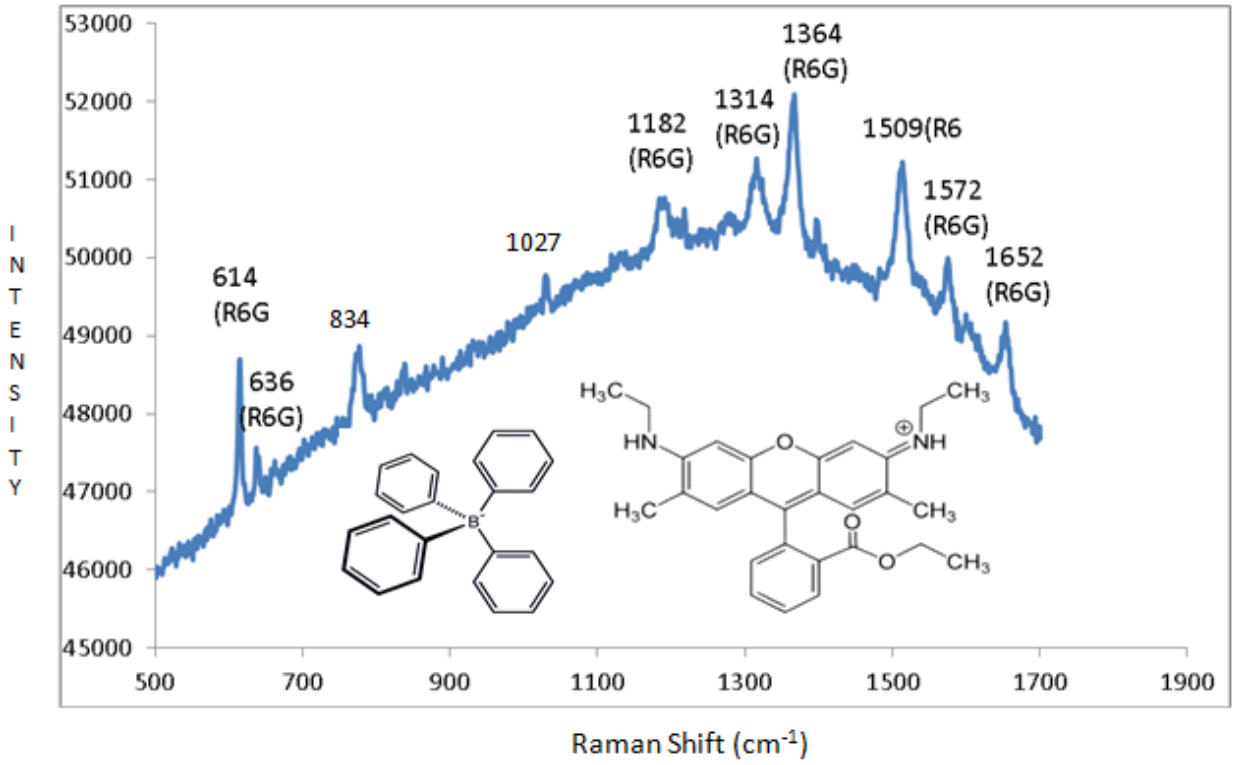

Figure 4.8: Raman spectra of R6G[TPB] nanowires on gold surface; Inset- R6G[TPB] molecular structure. [Appendix A]

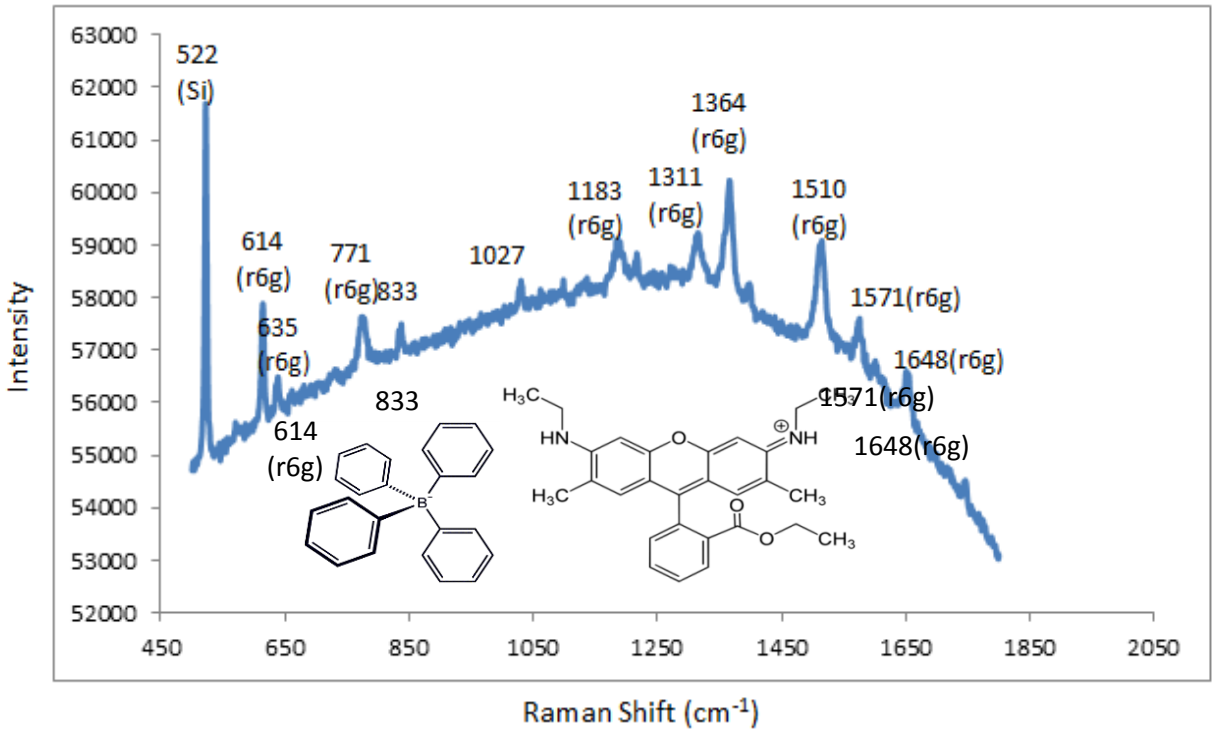

Figure 4.8: Raman spectra of R6G[TPB] nanowires on silicon surface. Inset- R6G[TPB] molecular structure. [Appendix A]

The second type of NanoGUMBOS, which we have used for Raman characterization, is Dimethylpyrollidinium bistrifluoromethanesulfonimide ($Py_{11}Tf_2N$). The preparation of this nanomaterial is discussed in Chapter 2. Figure 4.9 shows Raman spectra of $Py_{11}Tf_2N$ nanowires on silicon.

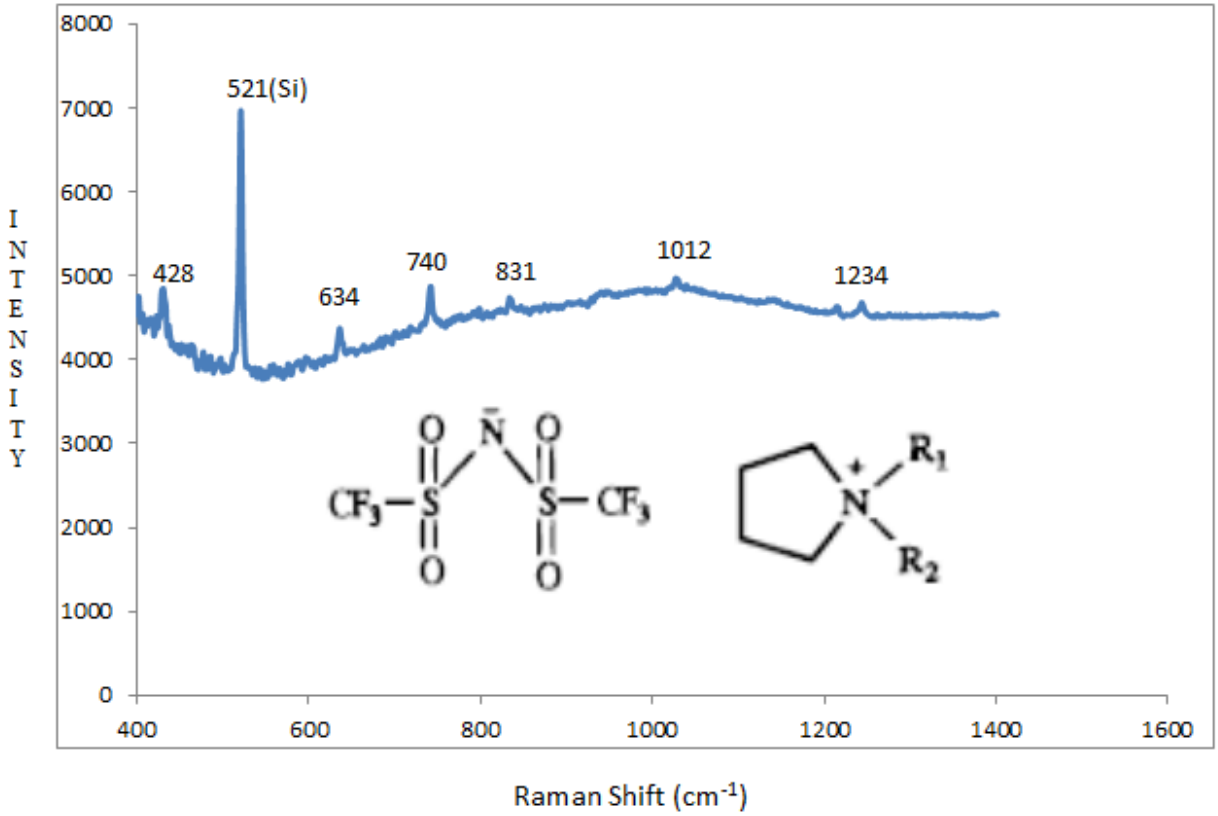

Figure 4.9: Raman spectra of $Py_{11}Tf_2N$ nanowires on silicon surface; Inset- $Py_{11}TF_2N$ structure. [Appendix A]

Raman peaks in the above figure correspond to the following chemical bonds [50][51]:

428cm^{-1} →(S-S)

634 cm^{-1} , 740 cm^{-1} →(C-S) aliphatic

1012 cm^{-1},1238 cm^{-1} →(C=S)

The third type of NanoGUMBOS we have used for Raman studies is PicopropylSH tetraphenylborate (ProMPyrSH[TPB]) nanorods on gold. Figure 4.10 shows Raman spectra of ProMPyrSH[TPB] nanorods on gold. The nanorods were coated with gold and again the Raman plot was obtained as shown in Figure 4.11. We observed some new peaks (not seen with bare nanorods) after coating the nanorods with gold. Also, the intensity of the peaks increased, which can be explained by the phenomenon of Surface Enhanced Raman Spectroscopy (SERS).

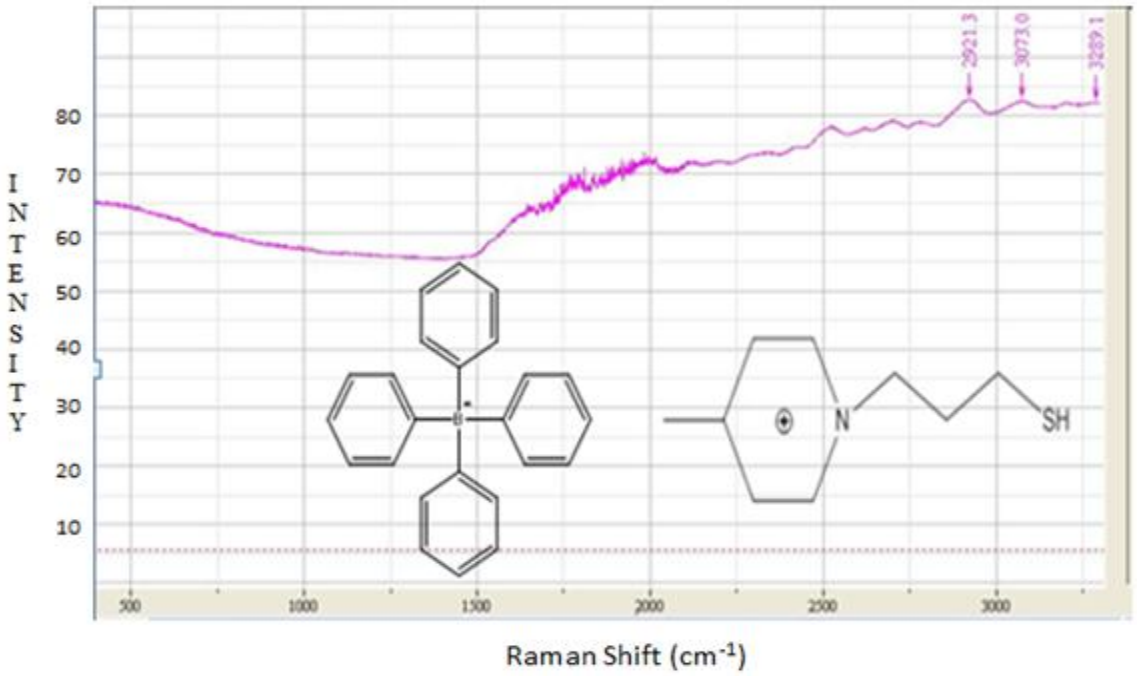

Figure 4.10: Raman spectra of ProMPyrSH[TPB] nanorods on gold surface; Inset - ProMPyrSH[TPB] structure. [Appendix A]

Raman peaks in the above figure correspond to the following chemical bonds [51]:

$2921cm^{-1}$ → (C-H)

$3073cm^{-1}$ → (=(C-H)

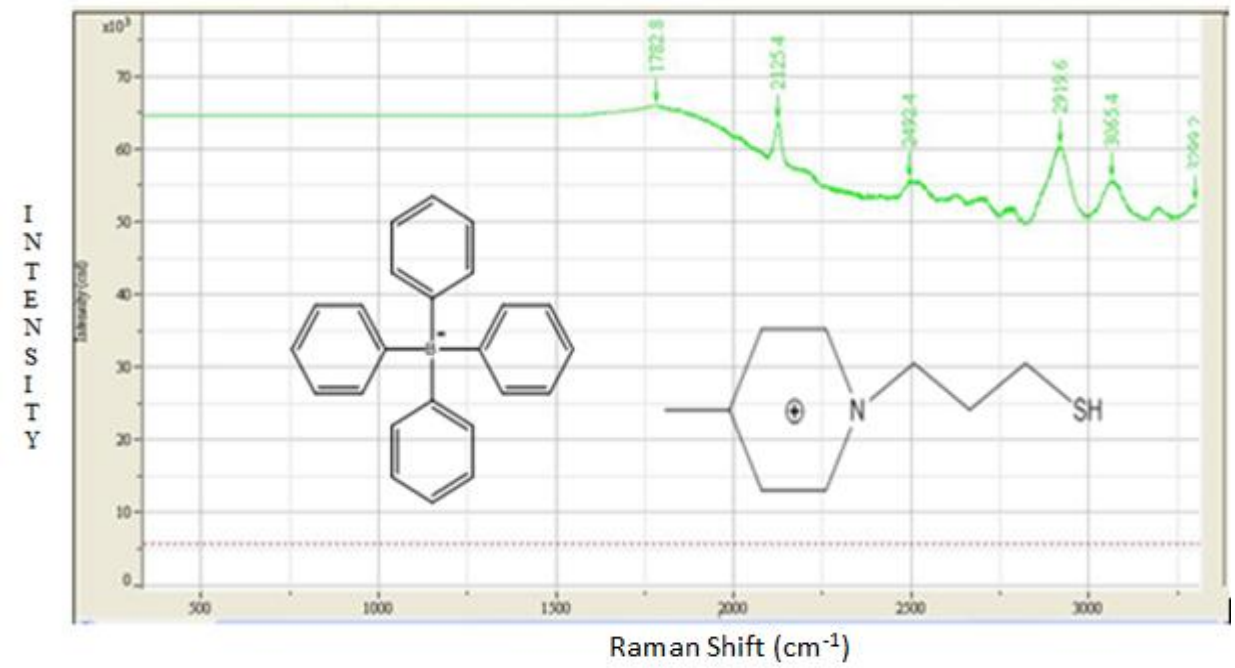

Figure 4.11: Enhancement of the Raman peaks on gold-coated ProMPyrSH[TPB] nanorods on gold; Inset - ProMPyrSH[TPB] structure. [Appendix A]

Raman peaks in the above figure correspond to the following chemical bonds [51]:

1782cm^{-1} → (C=C)

2125cm^{-1} → (C≡C)

2492cm^{-1} → SH

2919cm^{-1} → (C-H)

3065cm^{-1} → (=(C-H)

3299cm^{-1} → (≡(C-H))

4.6 Summary

In this chapter we have shown the Raman Spectroscopy of different types of NanoGUMBOS. The bands on the Raman spectra have been identified with respect to the chemical structure of each compound. The SERS enhancements of spectral peaks were observed after coating the NanoGUMBOS with gold. These results help in modeling the electron flow and interaction with phonons within the nanoparticles.

5. CONCLUSIONS

5.1 Summary

In this work, we characterized a new category of ionic liquids known as a Group of Uniform Materials Based on Organic Salts (GUMBOS). Synthesized by the Warner Group in the LSU Department of Chemistry, these materials represent a breakthrough in the creation of solid state ("frozen") nanoparticles. The unique properties and formation of NanoGUMBOS have been discussed. Different types of NanoGUMBOS, in terms of their anion-cation composition have been characterized using Atomic Force Microscopy (AFM) and Raman Spectroscopy (RS).

In the case of electrical characterization, a technique called Conductive Probe Atomic Force Microscopy (CP-AFM) was implemented. Conductivity was observed in all the types of NanoGUMBOS. The current-voltage (I-V) behavior and morphologies of each type of NanoGUMBOS are shown. The current magnitudes (for voltage range between -1V and +1V) of all types of NanoGUMBOS were found to be in the range of nano and pico amperes. The resistances of R6G[TPB], $Py_{11}Tf_2N$, PIC[NTF_2], PIC[BETI] were calculated to be 35M, 280M, 30G, 115G, respectively. As a first step in the study of Hybrid (organic-inorganic) Electronic Materials (HEMs), NanoGUMBOS were coated with gold, and the resultant I-V behavior was studied. We observed an increase in current (up to five orders of magnitude) after coating the nanorods with gold. The value of conductivity for each type of NanoGUMBOS can be calculated using the dimensions (determined from AFM imaging) and resistances (calculated from I-V plots).

Raman spectra of different types of NanoGUMBOS were studied and various peaks were identified. In case of R6G [TPB] nanowires, all the Raman peaks due to R6G molecule were

identified. Surface Enhanced Raman Spectroscopy (SERS) was observed on ProMPyrSH[TPB] nanorods. After gold-coating the ProMPyrSH[TPB] nanorods, some new peaks emerged and also the intensity of the Raman peaks increased. The chemical bonds corresponding to the Raman peaks were also identified.

5.2 Future Work

We have used CP-AFM method to study the electrical properties of NanoGUMBOS. Although, we have obtained the I-V signatures for different type of NanoGUMBOS, there is need for further study of electron transport mechanisms within the nanoparticles. The non-symmetric behavior and non-ohmic behavior of current can be explained with the help of molecular orientation within the nanoparticle. The oxidation and reduction processes in solid state GUMBOS have to be studied and compared with that of liquid state to understand the abrupt variations that are seen in the I-V curves. The electrical behaviors of each type of NanoGUMBOS can be related to devices like diodes, switches and resistors.

With respect to the implementation of CP-AFM measurements, tips having wear-resistant properties, smaller radius (below 10nm) can be used for better results. Capacitance and dielectric properties of NanoGUMBOS can also be determined using CP-AFM. The contact resistances at tip-nanoparticle and nanoparticle-gold junctions have to be determined for accurate calculation of electrical parameters.

Using Raman signatures of NanoGUMBOS, the vibrational states of the molecules can be determined. By combining the electron flow mechanism (determined by CP-AFM) and vibrational states of molecules (determined from Raman Spectroscopy results), the electron-phonon interaction within a single nanowire can be modeled. Techniques like “Tip enhanced

Raman Sectroscopy (TERS)," which combines the mechanisms of AFM, Raman Spectroscopy and SERS, can be used to get high resolution Raman images.

Fairly recently, nanowire transistors have shown electrostatic characteristics superior to silicon MOSFETS. [16] So, NanoGUMBOS can be used as a channel material in MOSFET. Figure 5.1 shows a basic model of a transistor with nanowire (red strip) as channel.

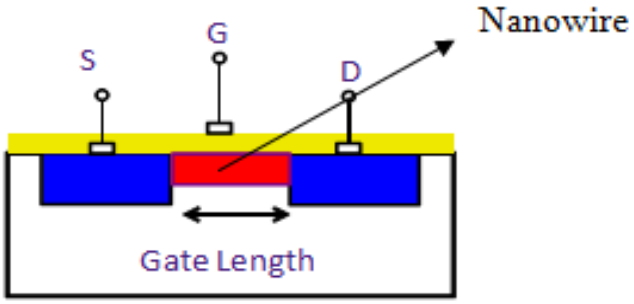

Figure 5.1: Illustration of a nanowire transistor.

Finally, the properties of NanoGUMBOS /HEMs can be utilized for possible applications in sensors, memory devices and opto-electronics.

BIBLIOGRAPHY

[1] (2010). *International Technology Roadmap for Semiconductors*. Available: http://www.itrs.net/

[2] G. E. Moore, "Cramming more components onto integrated circuits (Reprinted from Electronics, pg 114-117, April 19, 1965)," Proceedings of the IEEE, vol. 86, pp. 82-85, 1998.

[3] A. Aviram and M. A. Ratner, "Molecular Rectifiers," Chemical Physics Letters, vol. 29, pp. 277-283, 1974.

[4] F. Sawano, I. Terasaki, H. Mori, T. Mori, M. Watanabe, N. Ikeda, Y. Nogami, and Y. Noda, "An organic thyristor," Nature, vol. 437, pp. 522-524, 2005.

[5] J. R. Heath, "Molecular Electronics," Annual Review of Materials Research, vol. 39, pp. 1-23, 2009.

[6] A. Tesfai, B. El-Zahab, D. K. Bwambok, G. A. Baker, S. O. Fakayode, M. Lowry, and I. M. Warner, "Controllable formation of ionic liquid micro- and nanoparticles via a melt-emulsion-quench approach," Nano Letters, vol. 8, pp. 897-901, 2008.

[7] L. E. Foster, *Nanotechnology: Science, Innovation, and Opportunity*: Prentice Hall , 2005.

[8] M. Pagliaro, *Nano-age: how nanotechnology changes our future*: John Wiley & Sons, 2010.

[9] G. A. Horley, "The importance of being nano," Small, vol. 2, pp. 3-5, Jan 2006.

[10] P. Rodgers, *Nanoscience and Technology*: World Scientific Publishing, 2009.

[11] A. S. P. Vijay K. Varadan, Debashish Mukherji, *Nanoscience and Nanotechnology in Engineering*: World Scientific, 2010.

[12] B. Yu and M. Meyyappan, "Nanotechnology: Role in emerging nanoelectronics," Solid-State Electronics, vol. 50, pp. 536-544, 2006.

[13] G. Binning, H. Rohrer, C. Gerber, and E. Weibel, "Surface studies by Scanning Tunneling Microscopy," Physical Review Letters, vol. 49, pp. 57-61, 1982.

[14] A. Tsumura, H. Koezuka, and T. Ando, "Macromolecular electronic device - field-effect transistor with a polythiophene thin-film," Applied Physics Letters, vol. 49, pp. 1210-1212, 1986.

[15] K. Rupp and S. Selberherr, "The Economic Limit to Moore's Law," IEEE Transactions on Semiconductor Manufacturing, vol. 24, pp. 1-4, 2011.

[16] M. J. Kumar, M. A. Reed, G. A. J. Amaratunga, G. M. Cohen, D. B. Janes, C. M. Lieber, M. Meyyappan, L. E. Wernersson, K. L. Wang, R. S. Chau, T. I. Kamins, M. Lundstrom, B. Yu, and C. W. Zhou, "Guest Editorial Special Issue on Nanowire Transistors: Modeling, Device Design, and Technology," IEEE Transactions on Nanotechnology, vol. 7, pp. 643-650, 2008.

[17] C.Lee, WD.Fan, B.Lei, DH.Zhang, S.Han, T.Tang, XL.Liu, ZQ.Liu, S.Asano, M.Meyyappan, J.Han, Zhou, CW.Zhou, "Multilevel memory based on molecular devices," Journal of Nanoscience and Nanotechnology, vol. 84, pp. 1949-1951, 2004.

[18] G. Binning, C. F. Quate, and C. Gerber, "Atomic Force Microscope," Physical Review Letters, vol. 56, pp. 930-933, 1986.

[19] P. West. (2009). *Introduction to Atomic Force Microscopy- Theory Practise and Applications*. *2011*. Available: www.paulwestphd.com

[20] A. Avila and B. Bhushan, "Electrical Measurement Techniques in Atomic Force Microscopy, " Critical Reviews in Solid State and Materials Sciences, vol. 35, pp. 38-51, 2010.

[21] B. Q. Xu and N. J. J. Tao, "Measurement of single-molecule resistance by repeated formation of molecular junctions," Science, vol. 301, pp. 1221-1223, 2003.

[22] J. M. Beebe, V. B. Engelkes, B. S. Kim, J. D. Batteas, R. D. van Zee, and C. D. Frisbie, "Measurement of charge transport through self-assembled monolayers of organothiols by conducting probe atomic force microscopy," Abstracts of Papers of the American Chemical Society, vol. 230, pp. U1121-U1121, 2005.

[23] M. E. Greene, C. R. Kinser, D. E. Kramer, L. S. C. Pingree, and M. C. Hersam, "Application of scanning probe microscopy to the characterization and fabrication of hybrid nanomaterials," Microscopy Research and Technique, vol. 64, pp. 415-434, 2004.

[24] S. B. Kuntze, D. Ban, E. H. Sargent, S. J. Dixon-Warren, J. K. White, and K. Hinzer, "Electrical scanning probe microscopy: Investigating the inner workings of electronic and optoelectronic devices," Critical Reviews in Solid State and Materials Sciences, vol. 30, pp. 71-124, 2005.

[25] D. J. Wold and C. D. Frisbie, "Fabrication and characterization of metal-molecule-metal junctions by conducting probe atomic force microscopy," Journal of the American Chemical Society, vol. 123, pp. 5549-5556, 2001.

[26] J. Liang and G. Scoles, "An Analysis of Conductive-Probe Atomic Force Microscopy Applied to the Study of Electron Transport Mediating Properties of Self-Assembled Monolayers," Journal of Physical Chemistry C, vol. 114, pp. 10836-10842, 2010.

[27] L. C. Hsu, Y. Y. Li, and C. Y. Hsiao, "Synthesis, electrical measurement, and field emission properties of alpha-Fe2O3 nanowires," Nanoscale Research Letters, vol. 3, pp. 330-337, 2008.

[28] P. Birjukovs, N. Petkov, J. Xu, J. Svirksts, J. J. Boland, J. D. Holmes, and D. Erts, "Electrical Characterization of Bismuth Sulfide Nanowire Arrays by Conductive Atomic Force Microscopy," *Journal of Physical Chemistry C*, vol. 112, pp. 19680-19685, 2008.

[29] P. Gundersen, K. O. Kongshaug, E. Selvig, and R. Haakenaasen, "Electrical characterization of HgTe nanowires using conductive atomic force microscopy," Journal of Applied Physics, vol. 108, 2010.

[30] D. L. Jeanmaire and R. P. Vanduyne, "Surface Raman Spectroelectrochemistry .1. Heterocyclic, aromatic, and aliphatic-amines adsorbed on anodized silver electrode," Journal of Electroanalytical Chemistry, vol. 84, pp. 1-20, 1977.

[31] M. G. Albrecht and J. A. Creighton, "Anomalously intense raman-spectra of pyridine at a silver electrode," Journal of the American Chemical Society, vol. 99, pp. 5215-5217, 1977.

[32] S. M. Nie, "Probing single molecules and single nanoparticles by surface-enhanced Raman scattering," Abstracts of Papers of the American Chemical Society, vol. 221, pp. 110-PHYS, 2001.

[33] D. K. Bwambok, B. El-Zahab, S. K. Challa, M. Li, L. Chandler, G. A. Baker, and I. M. Warner, "Near- Infrared Fluorescent NanoGUMBOS for Biomedical Imaging," *Acs Nano*, vol. 3, pp. 3854-3860, 2009.

[34] A. Tesfai, B. El-Zahab, A. T. Kelley, M. Li, J. C. Garno, G. A. Baker, and I. M. Warner, "Magnetic and Nonmagnetic Nanoparticles from a Group of Uniform Materials Based on Organic Salts," *Acs Nano,* vol. 3, pp. 3244-3250, 2009.

[35] R. E. Del Sesto, T. M. McCleskey, A. K. Burrell, G. A. Baker, J. D. Thompson, B. L. Scott, J. S. Wilkes, and P. Williams, "Structure and magnetic behavior of transition metal based ionic liquids," Chemical Communications, pp. 447-449, 2008.

[36] R. D. Rogers and K. R. Seddon, "Ionic liquids - Solvents of the future?," Science, vol. 302, pp. 792-793, 2003.

[37] M. G. Del Popolo and G. A. Voth, "On the structure and dynamics of ionic liquids," Journal of Physical Chemistry B, vol. 108, pp. 1744-1752, 2004.

[38] I. M. Warner, "Nanogumbos: The next generation of nanomaterials," *Louisiana State University Dept.* of Chemistry Colloquium, Baton Rouge, LA, 2010.

[39] S. L. de Rooy, B. El-Zahab, M. Li, S. Das, E. Broering, L. Chandler, and I. M. Warner, "Fluorescent one-dimensional nanostructures from a group of uniform materials based on organic salts," *Chemical Communications,* vol. 47, pp. 8916-8918, 2011.

[40] S. Das, D. Bwambok, B. El-Zahab, J. Monk, S. L. de Rooy, S. Challa, M. Li, F. R. Hung, G. A. Baker, and I. M. Warner, "Nontemplated Approach to Tuning the Spectral Properties of Cyanine-Based Fluorescent NanoGUMBOS," *Langmuir*, vol. 26, pp. 12867-12876, 2010.

[41] I. Pacific Nanotechnology. (2002). *Nano-R™ AFM User's Manual*. Available: http://aries.ucsd.edu/LASERLAB/DIAG/nanoR_manual.pdf

[42] M. Radmacher, J. P. Cleveland, M. Fritz, H. G. Hansma, and P. K. Hansma, "Mapping Interaction forces with the Atomic-Force Microscope," Biophysical Journal, vol. 66, pp. 2159-2165, 1994.

[43] N. Siraj, Oxidation and Reduction process in GUMBOS ed, 2011.

[44] J. R Ferraro, K. Nakamoto, C.W. Brown, Introductory Raman spectroscopy, 2nd ed.: Academic Press, 2003.

[45] HORIBA, Ltd [Online]. Available: http://www.horiba.com/scientific/products/raman-spectroscopy/tutorial-faqs/raman-tutorial/raman-scattering/

[46] P. L. Stiles, J. A. Dieringer, N. C. Shah, and R. R. Van Duyne, "Surface-Enhanced Raman Spectroscopy," Annual Review of Analytical Chemistry, vol. 1, pp. 601-626, 2008.

[47] M. D. Michael A. Stroscio, *Phonons in Nanostructures*, illustrated ed.: Cambridge University Press, 2001.

[48] S. M. Nie and S. R. Emory, "Single-molecule detection and spectroscopy by surface-enhanced Raman scattering," Abstracts of Papers of the American Chemical Society, vol. 213, pp. 177-PHYS, 1997.

[49] Z. H. Zhou, L. Liu, G. Y. Wang, and Z. Z. Xu, "Surface-enhanced resonance Raman scattering spectroscopy of single R6G molecules," Chinese Physics, vol. 15, pp. 126-131, 2006.

[50] Mayo, Dana W., Miller, Foil A., Hannah, R. W - Course Notes on the Interpretation of Infrared and Raman Spectra. 2003

[51] Raman data and Analysis – www.horiba.com

APPENDIX A: PERMISSION TO USE COPYRIGHTED MATERIAL

A1.

Hello John,

The information you have sent was very helpfull in understanding the concepts in Raman Spectroscopy. As I am working on writing the thesis, one of the diagrams on Dispersive Raman Spectrometer - (13th slide in "Intro to Raman 2011.ppt") seems to be relevant to my work. Kindly looking forward to get your permission to use this figure in my thesis. Looking forward to hearing from you. Thanks in advance for your time and consideration

Sincerely,

Naveen
Graduate Research Assistant,
Dept of Electrical Engineering
Louisiana State University
Baton Rouge, LA-70803

---

chris.john@horiba.com <chris.john@horiba.com> 25 October 2011 19:58

To: Naveen Narayan Jagadish <nnaray2@tigers.lsu.edu>

Go for it
Just site Horiba accordingly
Good luck!!

A2.

Hello Sergio,

As I am working on writing my Master's thesis, I need to include some of your figures mentioned below:
1. Chemical structures of R6G[TPB] and Py11TF2N
2. SEM images of R6G[TPB] and Py11TF2N nanowires

Kindly looking forward to get your permission to use these figure in my thesis.

Thanks,

Naveen

Research Assistant,
Dept of Electrical Engineering
Louisiana State University
Baton Rouge, LA-70803

Sergio De Rooy <sderoo1@tigers.lsu.edu> 14 November 2011 12:10

To: Naveen Narayan Jagadish <nnaray2@tigers.lsu.edu>

Hi Naveen,

you have my permission. Good luck.

Best regards,

Sergio

A3.

Hello Ashleigh,

As I am working on writing my Master's thesis, I need to include some of your figures mentioned below:

1. Chemical structures of PicopropySH[TPB]
2. SEM images of ProMPyrSH[TPB] nanorods.

Kindly looking forward to get your permission to use these figure in my thesis.

Thanks,

Naveen
Research Assistant,
Dept of Electrical Engineering
Louisiana State University
Baton Rouge, LA-70803

Ashleigh Wright <awrig14@tigers.lsu.edu> 1 December 2011 10:20

To: Naveen Narayan Jagadish <nnaray2@tigers.lsu.edu>

Hello Naveen,

I give you permission for the use of the chemical structures and SEM images for the ProMPyrSH[TPB] nanorods.

Best wishes,

Ashleigh Wright

A4.

Hello Atiya,

As I am working on writing my Master's thesis, I need to include some of your figures mentioned below:
1. Chemical structures of PIC [NTF2] and BETI
2. SEM/TEM images of PIC [NTF2] and BETI
Kindly looking forward to get your permission to use these figure in my thesis.

Thanks,
Naveen
Research Assistant,
Dept of Electrical Engineering
Louisiana State University
Baton Rouge, LA-70803

Atiya Jordan <jordanan2@gmail.com> 14 November 2011 12:13

To: Naveen Narayan Jagadish <nnaray2@tigers.lsu.edu>

Naveen,

I give you permission to include the figures mentioned below in your Master's thesis.

Regards,

A5

Hello Rupp,

I am Naveen Jagadish, graduate student from Louisiana State University, Louisiana, USA. I am currently working on hybrid electronics regime and in the verge of completing my thesis chapters. I read the article cited: K. Rupp and S. Selberherr, "The Economic Limit to Moore's Law," Ieee Transactions on Semiconductor Manufacturing, vol. 24, pp. 1-4, Feb 2011. I would like to use the Figure 2 of page 3 in this article for my thesis literature review chapter. Kindly looking forward to get your permission to use is table in my thesis. Looking forward to hearing from you. Thanks in advance for your time and consideration

Sincerely,

Naveen
Research Assistant,
Dept of Electrical Engineering
Louisiana State University
Baton Rouge, LA-70803

Hi Naveen,

thanks for your email. I'm very pleased that you've considered my article, you can of course use the figure.

In principle, you also need to get the permission from the publisher. Since this can be tedious, I simply replotted the figure with different line styles again, so you can use the figures attached (eps and pdf) and don't need to fuzz with the publisher.

Best regards and good luck with your thesis,
Karli

A6

Naveen Narayan Jagadish <nnaray2@tigers.lsu.edu> 8 December 2011 11:36

To: chmyyl@ccu.edu.tw

Hello Sir/Madam,

I am Naveen Jagadish, graduate student from Louisiana State University, Louisiana, USA. I am currently working on hybrid electronics regime and in the verge of completing my thesis chapters. I read the article cited: L. C. Hsu, Y. Y. Li, and C. Y. Hsiao, "Synthesis, electrical measurement, and field emission properties of alpha-Fe2O3 nanowires," Nanoscale Research Letters, vol. 3, pp. 330-337, Sep 2008. I would like to use the Figure 5 (a) in this article for my thesis literature review chapter. Kindly looking forward to get your permission to use is table in my thesis. Looking forward to hearing from you. Thanks in advance for your time and consideration

Sincerely,

--
Naveen
Research Assistant,
Dept of Electrical Engineering
Louisiana State University
Baton Rouge, LA-70803

Yuan-Yao Li <chmyyl@ccu.edu.tw> 10 December 2011 20:33

To: Naveen Narayan Jagadish <nnaray2@tigers.lsu.edu>

Cc: andypolo20@yahoo.com.tw

Dear Mr Jagadis,

Thank you for your e-mail. It is OK to use the figure from my paper.

Best regards,

Yuan-Yao Li

APPENDIX B: WEAR ANALYSIS OF AFM TIP

Wear analysis of AFM tip before and after use

The SEM images of an AFM tip before and after CP-AFM measurements were compared and significant wear was observed. The Pt coating was peeled off and the tip no longer could be used for CP-AFM measurement as little current was flowing through it**.**

SEM images of tip before(left) and after wear

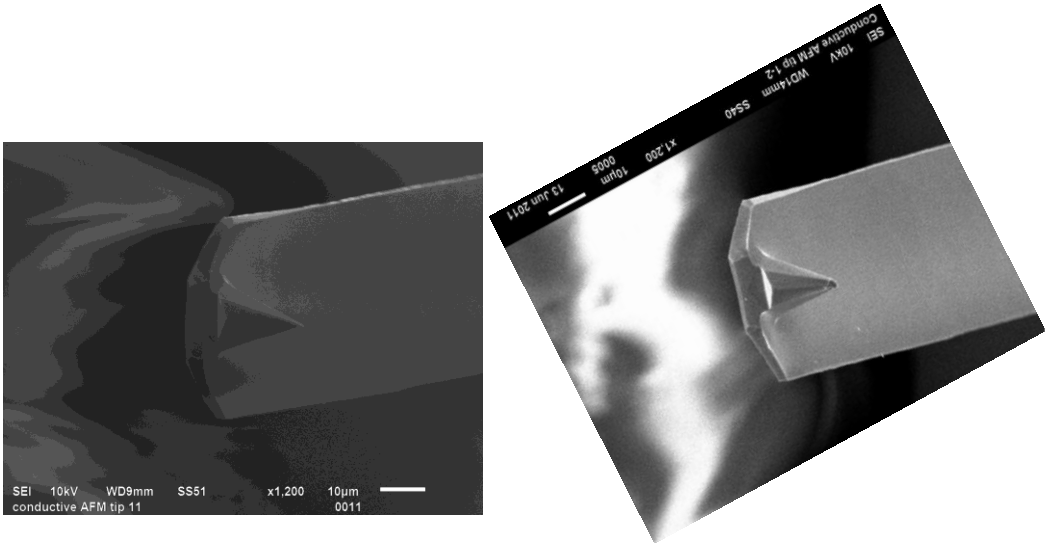

Figure : SEM images of unused Pt tip (left) and tip after imaging and sweeping voltage from -1V to 1V

APPENDIX C: INSTRUMENTATION OVERVIEW

Atomic Force Microscope (AFM) specifications:

Company: Pacific Nanotechnology (now Agilent)

Purpose: To get topographic image and electrical measurements.

Operation mode: Contact mode.

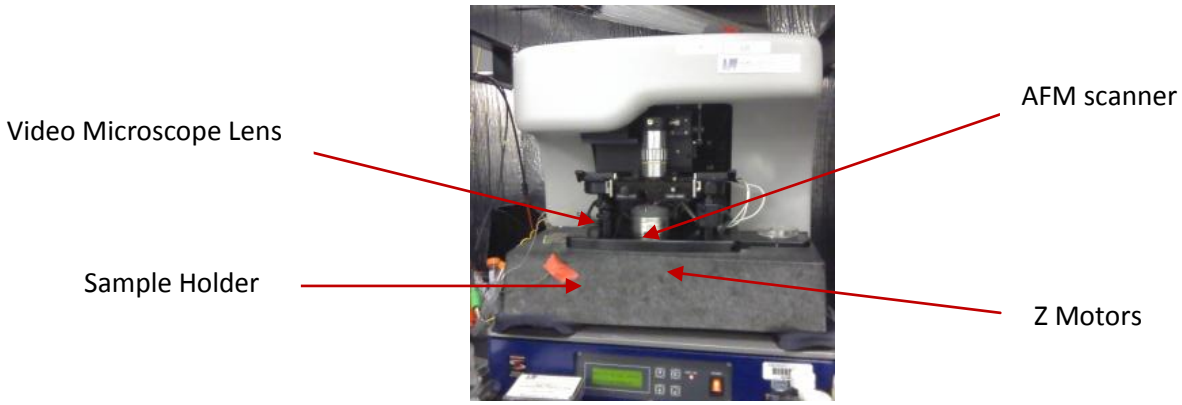

Figure 1: Pacific Nanotechnology (now Agilent) AFM

Semiconductor Characterization System specifications:

Company : Keithley

Model : 4200

The Model 4200 Semiconductor Characterization System (SCS) is an automated system to provide IV and CV characterization of semiconductor devices and test structures. Its advanced digital sweep parameter analyzer combines speed and accuracy for deep sub-micron characterization.

Tests are easily and quickly configured and run from the Keithley Interactive Test Environment (KITE). KITE is an application program designed and developed specifically for characterizing semiconductor devices and materials. Source and measurement functions for a test

are provided by up to eight Source-Measure Units (SMUs). Test capabilities are extended by support of a variety of external components.

Purpose: To obtain Current – Voltage (I-V) curves & Capacitance – Volatge(C-V) curves and thereby measure resistance, resistivity and conductance of the nanowires.

Operation mode: Voltage sweep (typically in the range of -2V to 1V)

Figure 2: Keithley 4200 SCS

AFM Probe specifications:

Company : Mikromasch

Low Noise conductive probe - DPE Ti-Pt/AlBS for imaging and cp-AFM measurements

Cantilever tip coated by continuous 30nm Pt film

Cantilever backside has 30-nm Aluminum coating.

Tip radius is < 40nm

Total tip height is 20-25 µm

Tip cone angle is 40 degrees

Resonant frequency is 12KHz

Force constant is 0.15N/m

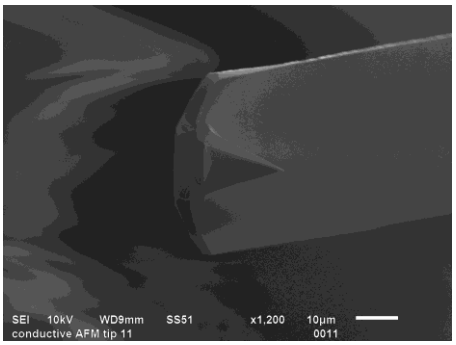

Figure 3: SEM image of DPE Ti-Pt/AlBS AFM tip from Mikromasch

VITA

Naveen Narayan Jagadish was born in Bangalore, India, in 1986. He obtained his Bachelor of Engineering degree in Telecommunication from Visvesvaraya Technological University, Belgaum, India, in Jun 2007. He is currently a candidate for Master of Science in Electrical Engineering at Louisiana State University, Baton Rouge, Louisiana.